New Method for the Determination of Figure of Merit ZT of Thermoelectric Devices

Bachelor Thesis

Albert Pergjokaj

Supervised by

Prof. Dr. Andreas Schilling

26.08.2021

Abstract

In order to measure the figure of merit ZT of a thermoelectric device, one has to measure the Seebeck coefficient, the total thermal conductivity and the internal electrical resistance separately which can be quite cumbersome. The standard method for measuring ZT involves at least two separate experiments.
This thesis describes new methods for measuring the figure of merit "ZT" using one single experiment. The new methods both require the same experimental setup. One side of the thermoelectric cooler is kept cool at room temperature while the other is heated up using a heat source. The heat source is then shut down and the body is left to cool and a measurement of the temperature decay is taken. If one measurement of the temperature decay is taken while the thermoelectric cooler is inactive and one measurement is taken while it is active, two time constants which describe the exponential decay of the temperature are obtained. The figure of merit ZT can then be obtained solely by using these two time constants, which means that nothing more than a temperature gradient is needed for the determination of ZT.

The measurement results obtained via the new methods were compared to the measurement results obtained by using the standard method and they are in good agreement with each other.

Contents

Introduction

1.1 Seebeck and Peltier effects

A thermoelectric device is a module, which converts heat into electrical energy and vice versa. This is done via the Seebeck and Peltier effect correspondingly.

The Seebeck effect was found by Thomas Seebeck in 1821 [1]. The Seebeck effect describes that when a material (a metal rod, for example) is heated up to a temperature T_H at one end and kept cool at a temperature T_C at the other end, a difference in the electrical potential appears between the cold and the hot end. This electrical potential can be described by the following equation:

$$\Delta V_S = \alpha \Delta T \ [V] \tag{1.1}$$

where α is an intrinsic property of the material, called Seebeck coefficient, given in $[V/K]$ and ΔT is the temperature difference $(T_H - T_C)$. This effectively allows for power generation, if able to keep the temperature gradient up. In order to be able to keep the temperature gradient up, it is usual to use junctions of two different materials with different Fermi-energies, as will be explained later in this chapter. One of the junctions is then heated up while the other is kept cool. A schematic view of the Seebeck effect can be seen in figure 1.1.

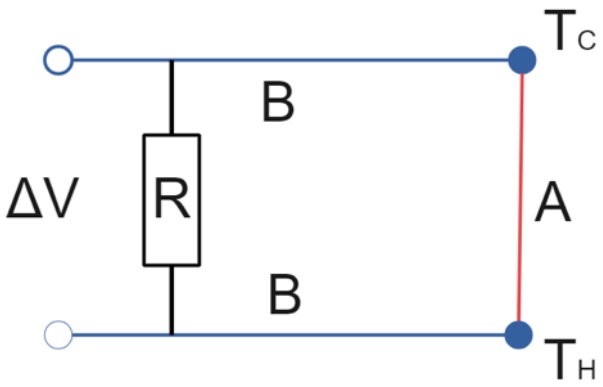

Figure 1.1: Schematic description of the Seebeck effect. "A" in red represents the first material, while "B" in blue represents the second material. The voltmeter between the two "B" materials measures the electrical potential due to the Seebeck effect.

This can be done with simple wires, which then can be used as a thermometer to determine ΔT according to equation (1.1). That is called a thermocouple.

The opposite can also be achieved, meaning that a temperature difference ΔT can be imposed by letting a current flow through the materials and their junctions. This allows the cooling of one junction while heating the other junction, similar to a refrigerator. Peltier found this effect in 1834, which is why it is called the Peltier effect [2,3]. A schematic view of the Peltier effect can be seen in figure 1.2.

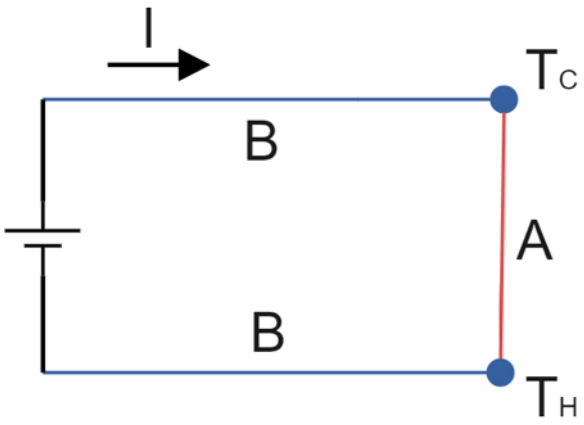

Figure 1.2: Schematic description of the Peltier effect. "A" in red represents the first material, while "B" in blue represents the second one. Driving a current through the circuit results in a temperature difference at the junctions of the materials.

These two effects can be better understood if we look at the Fermi levels and the energy bands. The electronic band structure for a metal can be seen in figure 1.3.

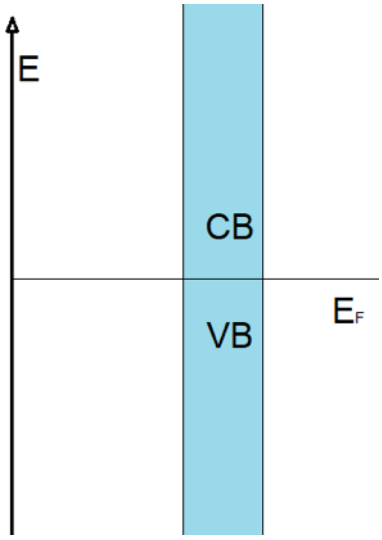

Figure 1.3: Electronic band structure of a metal. CB stands for conduction band and VB for valence band. E_F is the Fermi level.

The Fermi-Dirac distribution for electrons gives the probability of an electron occupying a state of energy E and is given by:

$$f_e(E,T) = \frac{1}{exp(\frac{E-E_F}{k_B T}) + 1} \tag{1.2}$$

where E is the energy of the electron, k_B is the Boltzmann constant and T is the temperature [4].

The Fermi-Dirac distribution for different temperatures can be seen in figure 1.4.

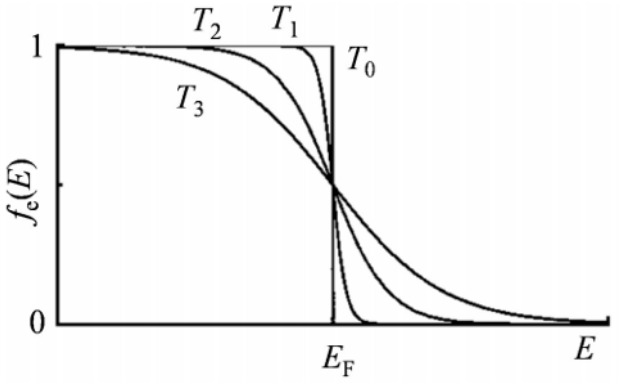

Figure 1.4: Fermi-Dirac distribution with $T_0 = 0K$ and $T_3 > T_2 > T_1 > T_0$. At T_0, all electrons are in the valence band as the probability of an electron occupying an energy state within the valence band is 1 [5].

The probability of an electron being in the conduction band instead of the valence band therefore rises, if the temperature rises.
If now one side of a metal rod is actively heated to T_H while the other side is kept cool at T_C, the probability that an electron is in the conduction band is higher on the hot end than on the cold end. There will be a noticeable concentration of electrons in the conduction band, above the Fermi energy on the hot end. As always, the principle of minimum energy applies and the charge carriers go to where the energy is lower, meaning they travel from the hot end to the cold end. In doing so, they also carry some of thermal energy with them. Now that there are more charge carriers on the cold side of the metal rod, there is an electrical potential difference from cold side to the hot side, proportional to the temperature difference between the two ends.

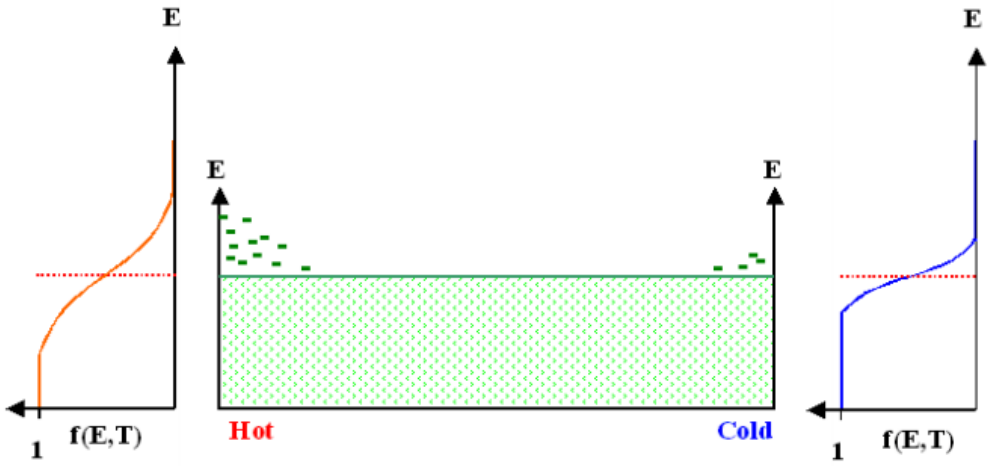

Figure 1.5: Metal rod which is hot on one end and cold on the other end. On the hot end, the Fermi-Dirac distribution is more eccentric than on the cold end, as the temperature is higher. This leads to electrons on the hot end having higher energies than on the cold end. The electrons then seek to lower their energy, meaning they travel to the cold end while carrying some thermal energy with them. The effect no longer holds when the metal rod is in thermal equilibrium [6].

A higher temperature also means higher momentum. This is critical for maintaining the temperature difference. In fact, the temperature difference cannot be maintained in the case described in figure 1.5, since the hot, high momentum electrons travel to the cold end of the rod faster than cold, low momentum electrons are able to diffuse towards the hot side of the rod. The solution to this problem is to lower the potential at the hot end and to raise it at the cold end. One method of achieving this would be to use a junction of two different metals which have different Fermi energies, instead of one single metal rod.
It should be noted that the explanation above has been simplified. In practise, the Fermi level is dependent on the temperature. Also, attaching one material to another ($E_{F,A} \neq E_{F,B}$) without any form of electrical insulation will result in an electrical potential difference, resulting in electrons from one material to flow into the other material, until the two Fermi levels are equalized [4, 7].

The Peltier effect can be explained by looking at a junction of a metal to a semiconductor, as seen in figure 1.6 [6].

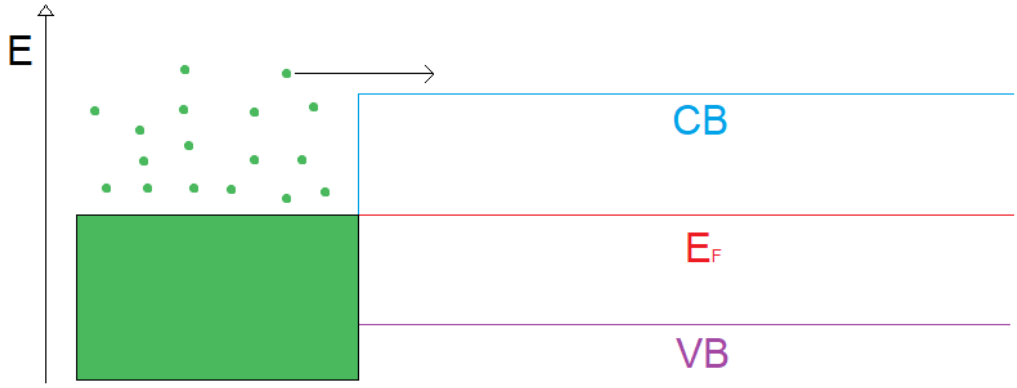

Figure 1.6: Junction between a metal (left) and a semiconductor (right). CB stands for conduction band, while VB stands for valence band. The green balls represent the free electrons of the metal. If now a current flowing from the metal to the semiconductor is applied, high energy electrons carrying thermal energy are transported to the conduction band of the semiconductor, resulting in a net transport of thermal energy out of the metal. The metal thus cools down. If the current is reversed, high energy electrons from the conduction band of the semiconductor are transported into the metal, resulting in the metal heating up [6]. In this case, the Fermi levels of the metal and semiconductor will not equalize, since we applied an external potential difference which prevents this [8].

It is important to note that the thermoelectric phenomena are both accompanied by the irreversible effects of thermal conduction and Joule heating. It is not possible to drive an arbitrarily high current through a thermoelectric cooler, since at some point, the Joule heating which is given by $P_J = RI^2$ will be greater than the cooling power due to the Peltier effect given by $P_P = \alpha TI$ [9, 10].

In practise, p-type and n-type semiconductors are the preferred materials to make use of the Seebeck and Peltier effect instead of metals. This is done in order to maximize the efficiency of the device. A power generation device, fueled by the Seebeck effect, schematically looks like figure 1.7, while a refrigeration device, fueled by the Peltier effect, schematically looks like figure 1.8 [11].

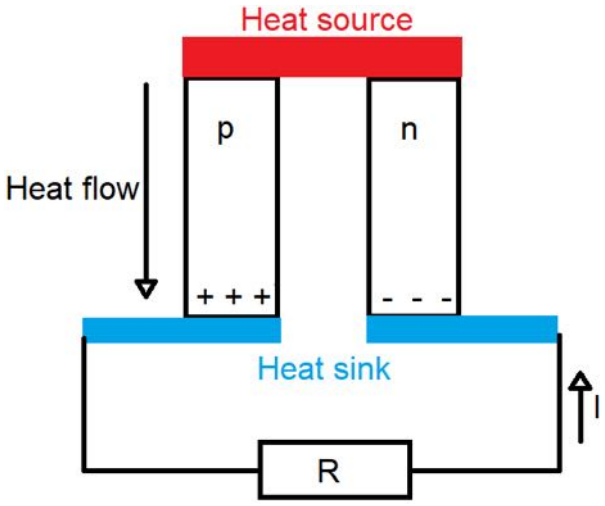

Figure 1.7: Schematic description of the Seebeck effect used for power generation. A heat source is placed on top of the p-type and n-type semiconductors, leading to a downwards flow of the charge carriers, which also carry thermal energy. Since there is an excess of positively charged holes on the p-type side and an excess of negatively charged electrons on the n-type side, there is a net potential difference ΔV_S which causes a current I to flow through the resistance R.

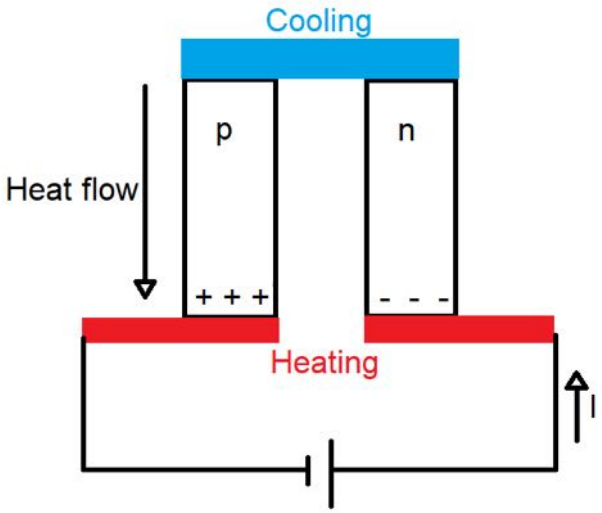

Figure 1.8: Schematic description of the Peltier effect used for cooling. Driving a current through the n-type semiconductor causes electrons carrying thermal energy to flow towards the bottom. The current then goes downwards through the p-type semiconductor, causing holes carrying thermal energy to flow towards the bottom as well. The result is that the top side of the p-type and n-type semiconductors is cooled, while the bottom side is heated. The sides which are cooled and heated can be swapped by reversing the flow of the current.

To further maximize this effect, it is usual to build many such p-type and n-type semiconductor cubes, such that they are connected in series electrically and in parallel thermally, as seen in figure 1.9 [12].

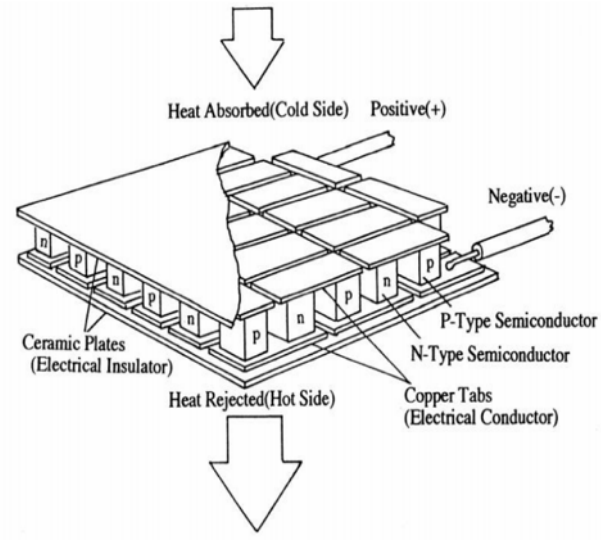

Figure 1.9: Inside view of a thermoelectric cooling device as it is used in practise [12].

1.2 Figure of Merit ZT

The figure of merit ZT is a dimensionless value which is directly related to the efficiency of the thermoelectric device. It is given by the following equation:

$$ZT = \frac{\alpha^2 \sigma T}{k} = \frac{\alpha^2 T}{Rk} \tag{1.3}$$

where α is the Seebeck coefficient, σ the electrical conductivity, T the temperature, k the total thermal conductivity in the dimensions $\left[\frac{W}{K}\right]$ and R the internal electrical resistance, obtained by using $R = \frac{1}{\sigma}$.

The relation between the efficiency and the figure of merit is seen in the equation below:

$$\eta = \frac{W}{Q_H} = \frac{T_H - T_C}{T_H} \left[\frac{\sqrt{1 + ZT_{avg}} - 1}{\sqrt{1 + ZT_{avg}} + T_C/T_H} \right] \tag{1.4}$$

where W is the power input, Q_H is the net heat flow rate, T_H is the temperature on the hot end, T_C is the temperature on the cold end and T_{avg} is the average temperature. The higher the figure of merit, the more efficient the device, since $\eta \propto \sqrt{1 + ZT_{avg}}$. This explains why semiconductors are used in practise, rather than metals. For the figure of merit to be as large as possible, the electrical conductivity needs to be large while the thermal conductivity needs to be small. This is more feasible to achieve in semiconductors, which is why they are preferred instead, among other reasons.
The figure of merit can be further increased by using two different materials (e.g. p-type and n-type semiconductors), as ZT for two materials is expressed by the following equation:

$$ZT = \frac{(\alpha_p - \alpha_n)^2 T}{\sqrt{R_p k_p} + \sqrt{R_n k_n}} \tag{1.5}$$

As can be seen, the larger the difference between the two Seebeck coefficients of the p-type and n-type semiconductors, the higher ZT [2].

The standard procedure to measure ZT is quite cumbersome, as it requires two separate experiments [13]. In this thesis, I will show that ZT can be measured in one single experiment. The theory of this new method will be elaborated in the next chapter.

Theory

2.1 First Method: Temperature Independent ZT

The flow of heat of a thermoelectric cooler is described in the following set of equations [10]:

$$Q_C = -\alpha T_C I + \frac{1}{2} R I^2 - k(T_H - T_C) \tag{2.1}$$

$$Q_H = \alpha T_H I + \frac{1}{2} R I^2 + k(T_H - T_C) \tag{2.2}$$

where Q_C is heat removed from the side of the cooler which is to be cooled and Q_H is the heat rejected at the other side of the cooler, according to figure 1.8. The middle term $\frac{1}{2}RI^2$ comes from the Joule heating due to the internal resistance of the cooler $P = RI^2$. It has been assumed that the Joule heating distributes equally to the cool side and to the hot side [14].
If we do not drive a current through the cooler after heating up the cooling side to T_H while keeping the other side at T_C (by attaching a heat sink, for example) and then remove the heat source and let the heated side cool down once T_H is reached and the heat sink assumed to be an infinite thermal reservoir, such that $T_C = const.$, while also assuming that the thermal conductivity k and the heat capacity C are not temperature dependent, equation (2.1) reduces to:

$$Q_C = -k(T_H - T_C) \tag{2.3}$$

A schematic of this process can be seen in figure 2.1.

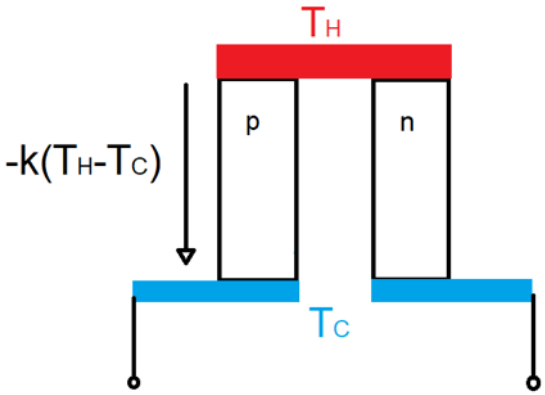

Figure 2.1: Process of cooling down when the thermoelectric cooler is inactive. The only term which contributes to the heat flow is $Q_C = -k(T_H - T_C)$.

Using $Q_C = C\dot{T}_H$, we get:

$$C\dot{T}_H = -k(T_H - T_C) \tag{2.4}$$

$$\int dT_H \frac{1}{(T_H - T_C)} = -\frac{k}{C}\int dt \tag{2.5}$$

$$log(T_H(t) - T_C) = Aexp\left(-\frac{k}{C}t\right) \tag{2.6}$$

$$T_H(t) = Aexp\left(-\frac{t}{C/k}\right) + T_C \tag{2.7}$$

Looking at equation (2.7), we are able to define the first time constant τ_1:

$$\tau_1 := C/k \tag{2.8}$$

By imposing the fact that $T_H(t=0) \stackrel{!}{=} T_H$, we can solve for the integration constant A:

$$T_H = A + T_C \tag{2.9}$$

$$A = T_H - T_C = \Delta T \tag{2.10}$$

Thus, the final expression for $T_H(t)$ becomes:

$$T_H(t) = \Delta T exp\left(-\frac{t}{\tau_1}\right) + T_C \tag{2.11}$$

Now the case is considered where the circuit is closed after heating up the cooled side to T_H, such that an internal current I runs through the thermoelectric cooler due to the Seebeck effect. The heat source is again removed once T_H is reached, letting the cooled side cool down. A schematic of this process can be seen in figure 2.2

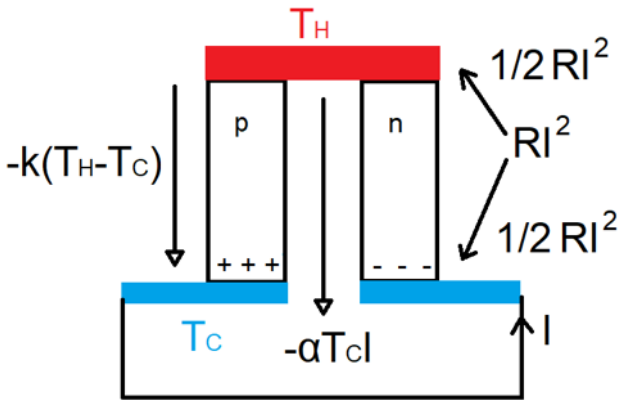

Figure 2.2: Process of cooling down when the thermoelectric cooler is inactive. If we neglect the Joule heating, the terms which contribute to the heat flow are $Q_C = -\alpha T_C I - k(T_H - T_C)$.

Using Kirchhoff's voltage law, which states that the sum of all voltages is equal to zero in a closed circuit we get a different equation for $T_H(t)$. Using equation (1.1) and

$\Delta V_R = RI$, we get [10, 15]:

$$\sum_{n=1}^{N} V_n = 0 \tag{2.12}$$

$$\Delta V_S - \Delta V_R = 0 \tag{2.13}$$

$$\alpha(T_H - T_C) - RI = 0 \tag{2.14}$$

$$T_H = \frac{RI}{\alpha} + T_C \tag{2.15}$$

Taking the derivative of equation (2.15) with respect to time, allows us to replace $\dot{T}_H$ in $Q_C = C\dot{T}_H$ from equation (2.1). This way, a differential equation for the internal current I is obtained:

$$\dot{T}_H = \frac{R}{\alpha}\dot{I} \tag{2.16}$$

$$\frac{CR}{\alpha}\dot{I} = -\alpha T_C I + \frac{1}{2}RI^2 - \frac{kR}{\alpha}I \tag{2.17}$$

$$CR\dot{I} + (\alpha^2 T_C + kR)I - \frac{1}{2}RI^2 = 0 \tag{2.18}$$

where equations (2.16) and (2.15) have been used in (2.1) to obtain (2.17).

Equation (2.18) can further be simplified by neglecting the Joule heating term $\frac{1}{2}RI^2$. This is plausible due to equation (2.14), since $\frac{1}{2}RI^2 < RI^2 = \alpha(T_H - T_C)I << \alpha T_C I$ if $T_H - T_C << T_C$. [10].
We end up with the following equation:

$$RC\dot{I} + (\alpha^2 T_C + kR)I \approx 0 \tag{2.19}$$

We can now solve this differential equation to obtain an expression for $I(t)$:

$$\frac{\dot{I}}{I} = \frac{-\alpha^2 T_C - kR}{RC} \tag{2.20}$$

$$\int \frac{1}{I} dI = \int \frac{-\alpha^2 T_C - kR}{RC} dt \tag{2.21}$$

$$log(I(t)) = A\frac{-\alpha^2 T_C - kR}{RC}t \tag{2.22}$$

$$I(t) = Aexp\left(\frac{-\alpha^2 T_C - kR}{RC}t\right) \tag{2.23}$$

Equation (2.23) can then be used to replace I in equation (2.14). This ultimately allows us to obtain an expression for T_H for an active thermoelectric cooler:

$$\alpha(T_H(t) - T_C) - RAexp\left(\frac{-\alpha^2 T_C - kR}{RC}t\right) = 0 \tag{2.24}$$

$$T_H(t) = A\frac{R}{\alpha}exp\left(\frac{-\alpha^2 T_C - kR}{RC}t\right) + T_C \tag{2.25}$$

The integration constant A can again be identified by imposing the fact that $T_H(t=0) \stackrel{!}{=} T_H$:

$$T_H = A\frac{R}{\alpha} + T_C \tag{2.26}$$

$$A = \frac{\alpha}{R}(T_H - T_C) \tag{2.27}$$

$$T_H(t) = \Delta T exp\left(\frac{-\alpha^2 T_C - kR}{RC}t\right) + T_C \tag{2.28}$$

By defining a second time constant τ_2, it is possible to express the exponential decay, analogue to equation (2.11):

$$T_H(t) = \Delta T exp\left(-\frac{t}{\tau_2}\right) + T_C \tag{2.29}$$

with

$$\tau_2 := \frac{RC}{\alpha^2 T_C + kR} \tag{2.30}$$

$$= \frac{C/k}{1 + \frac{\alpha^2 T_C}{Rk}} \tag{2.31}$$

$$= \frac{\tau_1}{1 + ZT} \tag{2.32}$$

where $\tau_1 = C/k$ and $ZT = \frac{\alpha^2 T_C}{Rk}$ have been used in equation (2.31) in order to obtain (2.32).

Thus, we can finally obtain an expression for ZT by solving for it in equation (2.32):

$$\boxed{ZT = \frac{\tau_1}{\tau_2} - 1} \tag{2.33}$$

It is therefore possible to determine ZT simply through a temperature gradient, namely by measuring the exponential decay of the temperature of the heated body, once where the thermoelectric cooler is inactive (τ_1, circuit open) and once where it is active (τ_2, circuit closed), while the heat sink is kept at a constant temperature T_C.

Time constants τ_1 and τ_2 can also be obtained by heating up the side which is to be cooled down by the thermoelectric cooler and measuring the rise of the temperature over time. Since this is the opposite of the process described above, we can take equations (2.11) and (2.29) and write:

$$T'_H(t) = \Delta T\left(1 - exp\left(-\frac{t}{\tau'_{1,2}}\right)\right) + T_C \tag{2.34}$$

This makes sense, considering $T'_H(t=0) = T_C$ and $T'_H(t \to \infty) = \Delta T + T_C = T_H$ Time constants τ'_1 and τ'_2 have been marked with a prime, because they are only equivalent to τ_1 and τ_2 if the time constants are truly temperature independent. Since ZT explicitly depends on the temperature from equation (1.3), while also depending on α, R and k, which all depend on temperature too [16], it is highly unlikely that the time constants τ_1 and τ_2 are truly constant and do not depend on temperature as well.

2.2 Second Method: Temperature Dependent ZT

If we can therefore find a way to express $\tau_{1,2}$ not as constants, but dependent on temperature T, we can also find the temperature dependence of ZT itself according to equation (2.33).

Assuming our body which is to be cooled down by the thermoelectric cooler has an isotropic temperature at any time t (not dependent on spatial coordinates) and that heat exclusively flows from the hot body into the heat sink, neglecting any thermal radiation and other effects, this is indeed achievable. The first law of thermodynamics for a closed system states the following:

$$\dot{Q} = W\kappa + \frac{dU}{dt} \tag{2.35}$$

where $\dot{Q}$ is the heat transfer rate, $W\kappa$ the work transfer rate and $\frac{dU}{dt}$ the change of the internal energy per time.
Assuming no work is done on the system, this reduces to [17]:

$$\dot{Q} = \frac{dU}{dt} \tag{2.36}$$

Using $dQ = CdT$ [18], equation (2.36) becomes as follows:

$$\dot{Q} = \frac{dU}{dt} = C\frac{dT}{dt} \tag{2.37}$$

Fourier's law of heat conduction states:

$$\frac{\dot{Q}}{A} = -\kappa\frac{dT}{dx} \tag{2.38}$$

where $\frac{Q}{A}$ is the heat flux (heat rate per unit area) and κ the thermal conductivity in units of $\left[\frac{W}{mK}\right]$ [17].
Inserting equation (2.37) into equation (2.38), the following expression is obtained:

$$\frac{C}{A}\frac{dT}{dt} = -\kappa\frac{dT}{dx} \tag{2.39}$$

$$\dot{T} = -\frac{\kappa A}{C}\frac{dT}{dx} \tag{2.40}$$

$$\dot{T} = -\frac{k}{C}\Delta T \tag{2.41}$$

$$\dot{T_H} = -\frac{1}{\tau}(T_H(t) - T_C) \tag{2.42}$$

where $\tau = \frac{C}{k}$ was used to obtain equation (2.42) and $k = \frac{\kappa A}{dx}$ was used to obtain the total thermal conductivity k in units of $[W/K]$. Solving for τ therefore gives us an expression for temperature dependent time constants:

$$\tau_{1,2} = \frac{T_C - T_H(t)}{\dot{T}_H} \tag{2.43}$$

Finally, we are able to determine a temperature dependent ZT via equation (2.33).

It should be noted that the actual value of the heat capacity C is not relevant for anything other than tweaking the values of τ, as seen in equations (2.8) and (2.41).

2.3 Third Method: Determining ZT using the Electrical Resistance R

A third and final method for determining ZT involves the electrical resistance R. When a current I is flowing through a thermoelectric cooler, heat is generated or absorbed (depending on the direction of the current) at rate $\dot{Q}$ as follows [10]:

$$\dot{Q} = \alpha T I \tag{2.44}$$

According to equation (2.38), we can then write:

$$\dot{Q} = \pm k \Delta T \tag{2.45}$$

$$\Delta T = \pm \frac{\dot{Q}}{k} \tag{2.46}$$

where the sign is either positive or negative depending on the direction of the current. We can decide to set the sign positive without a loss of generality.
Using this identity of ΔT in the equation for the Seebeck effect, we get:

$$\Delta V_S = \alpha \Delta T = \frac{\alpha^2 T}{k} I \tag{2.47}$$

If we now divide by I, we realize that we effectively measure a "false" electrical resistance R_{eff} when we naively drive a current through the thermoelectric cooler to measure its internal resistance:

$$\frac{\Delta V_S}{I} = \frac{\alpha^2 T}{k} = ZT * R_{TE} \tag{2.48}$$

$$R_{eff} = ZT * R_{TE} \tag{2.49}$$

where R_{TE} denotes the real internal electrical resistance of the thermoelectric cooler. This means that when we drive a current I through a thermoelectric cooler in order to measure its internal electrical resistance, we actually measure a resistance which is false, namely the effective electrical resistance R_{eff}. The actual measured voltage and electrical resistance are given by [19]:

$$V_{eff} = I * R_{TE} + V_S \tag{2.50}$$

$$R_{eff} = \frac{V_{eff}}{I} = R_{TE} + ZT * R_{TE} \tag{2.51}$$

$$R_{eff} = R_{TE}(1 + ZT) \tag{2.52}$$

Thus, once R_{TE} and R_{eff} are known, ZT can be obtained by solving for it in equation (2.52):

$$ZT = \frac{R_{eff}}{R_{TE}} - 1 \tag{2.53}$$

This could also potentially yield a new method for measuring the internal electrical resistance R_{TE} of a thermoelectric cooler. If equation (2.53) is set equal to (2.33), we obtain:

$$\frac{R_{eff}}{R_{TE}} = \frac{\tau_1}{\tau_2} \tag{2.54}$$

$$R_{TE} = \frac{R_{eff} * \tau_2}{\tau_1} \tag{2.55}$$

Experiment

3.1 Experimental Setup

The experiment itself can be seen in figure 3.1.

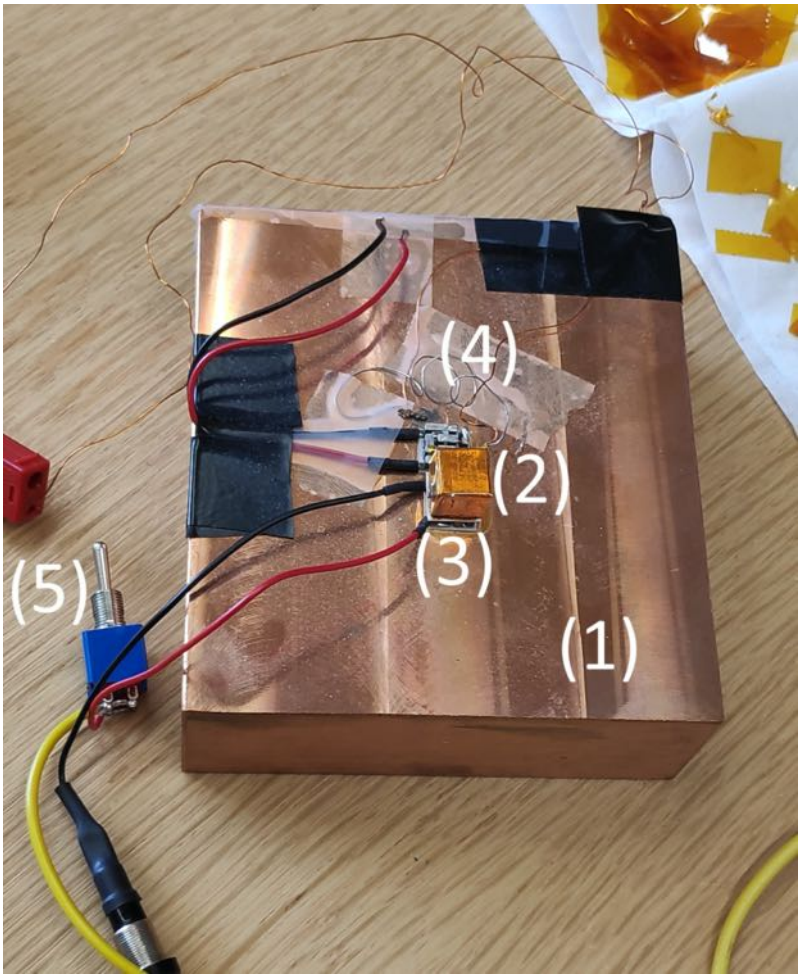

Figure 3.1: Experiment used for measurement of ZT. (1): Heat sink, approximated to be an infinite thermal reservoir such that $T_C \approx const$. It is a large body of copper. (2): Body on which a temperature T_H will be applied. It is also made of copper and much smaller than the heat sink. (3): Thermoelectric cooler, located beneath the smaller copper body (2). (4): Copper/Constantan (Type T) thermocouple used as a thermometer to measure $T_H - T_C$. Its junction is attached to the smaller copper body (2) via silver epoxy. The copper wire is directly connected to a voltmeter. The constantan wire is soldered onto the heat sink (1). From that solder joint, a copper wire is continued and connected to the voltmeter. (5): Switch used for activating (closed circuit) and deactivating (open circuit) the thermoelectric cooler (3).

It makes sense to approximate the temperature of the heat sink (1) as $T_C \approx const.$, considering the difference in mass of the copper body which is heated up to a temperature T_H: $m_{(1)} >> m_{(2)}$. This leads to the fact that the heat capacity of the heat sink is much larger than that of the small copper body: $C_{(1)} >> C_{(2)}$ due to $C = cm$, where c is the specific heat capacity [18]. The temperature of the heat sink has been set to room temperature for the experiment: $T_C = 295K$.

At the very beginning of the experiment, a soldering iron was used at low power in order to heat up the small copper body. However, this did not work very well as the heat dissipated too quickly and I was not able to build up a significant temperature gradient. An accident also occurred once, where I slipped with the soldering iron from the small copper body onto the silver epoxy adhesive, which caused the copper/constantan thermocouple to detach from the small copper body. This had to be cleaned up and re-glued with silver epoxy.
In order to get a meaningful temperature gradient and to prevent further accidents, a heater with $R_H = 10\Omega$ was ordered, which means that a heating power of $P_H = R_H I^2$ could be achieved by driving a current I through it. The heater can be seen in figure 3.2.

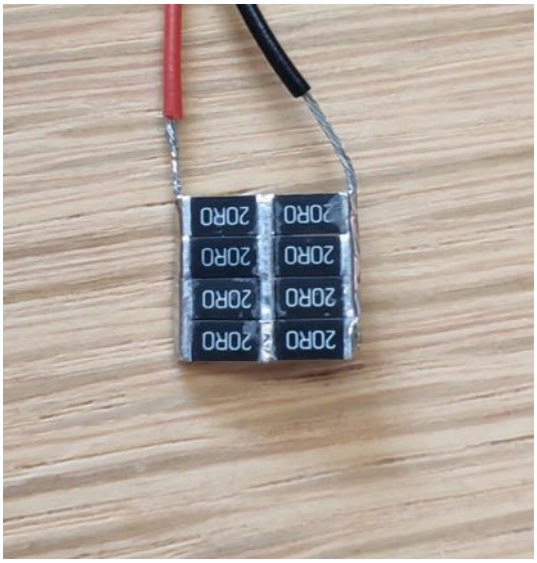

Figure 3.2: Heater which was attached to the small copper body. It consists of eight separate resistances with $R = 2\Omega$, adding up to a total of $R_H = 10\Omega$.

Before the heater could be soldered onto the small copper body, the place where the heater would be attached had to be electrically insulated first to prevent a short circuit. To do this, a heat resisting insulation tape was attached to the top of the small copper body. It can be seen as an orange film on top of the small copper body in figure 3.1.
A close up of the small copper body with its heater can be seen in figure 3.3.

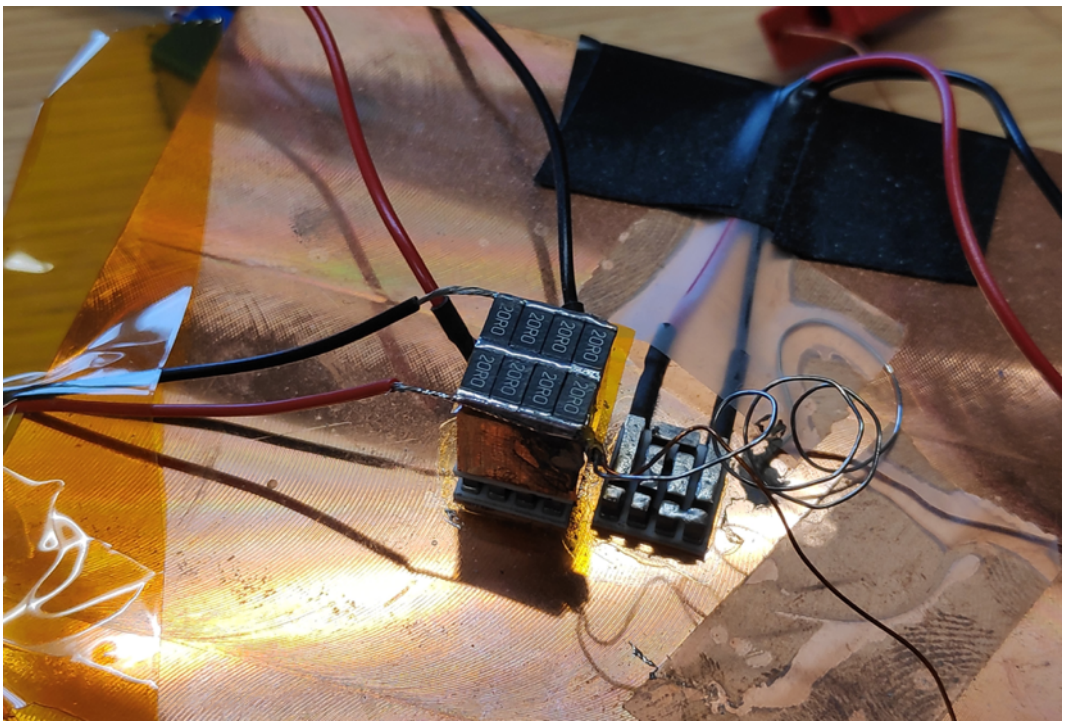

Figure 3.3: Close up of the experiment with the heater attached onto the small copper body. The thermoelectric cooler as well as the silver epoxy adhesive can be seen more clearly in this figure. The device on the right is a broken thermoelectric cooler, originating from a past experiment.

The experimental station can be seen in its entirety in figure 3.4.

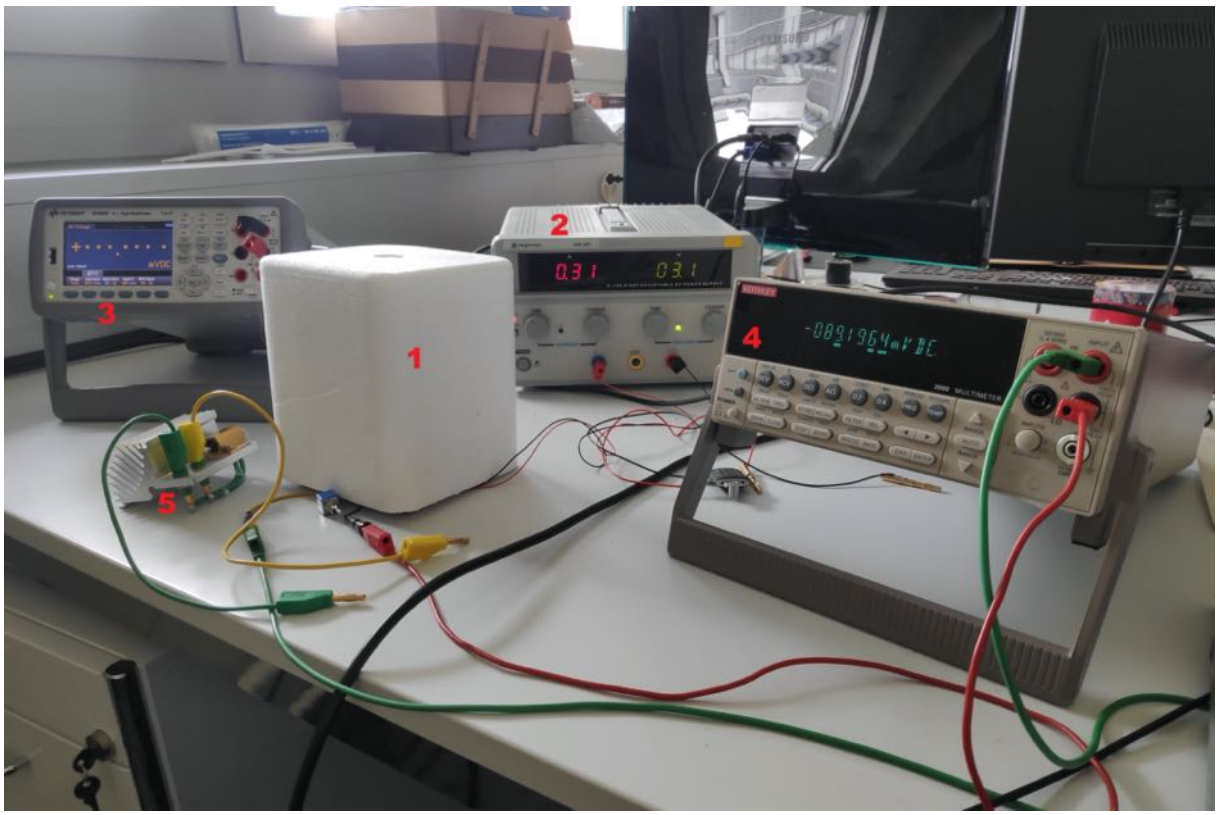

Figure 3.4: Experimental station. (1): Experiment described in figure 3.1, covered beneath a Styrofoam container for thermal insulation. (2): Power supply used to drive a current through the heater. Model: *Skytronic 650.682*. (3): First multi meter, used as a volt meter to measure $\Delta T = T_H - T_C$. This is where the two ends of the copper/constantan thermocouple connect to. The multi meter is connected to a computer via USB for data logging. Model: *Keysight 34465A*. (4): Second multi meter used as a volt meter. This is used in later stages of the experiment, where ZT was determined by measuring α, R_{TE} and k separately in order to compare it to the new method of measuring ZT. Model: *Keithley 2000*. (5): Load resistance $R_{Load} = 1\Omega$ used in later stages of the experiment in order to determine R_{TE}. (4) and (5) are not needed to measure ZT via the new method.

The software used for data logging is called *PathWave Digital Multimeter*.

3.2 Voltage to Temperature Conversion

Before anything can be measured, the voltages ΔV of the copper/constantan thermocouple have to be converted into temperature differences ΔT. To do this, my supervisor Prof. Dr. Schilling supplied me with a table which relates ΔV to $\Delta T = T_H - T_C$ when T_C is kept constant at $T_C = 295K$.
I plotted the measurement results given by the table and fitted a polynomial of degree two for it. The result can be seen in figure 3.5.

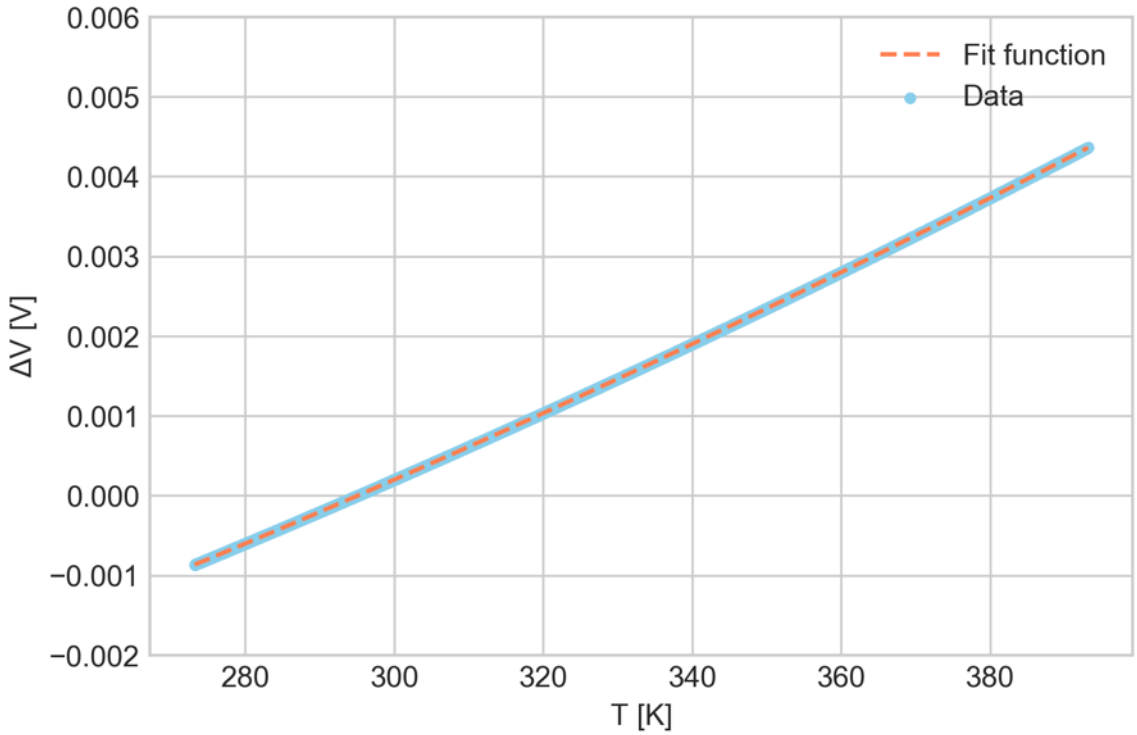

Figure 3.5: Conversion of voltage to temperature for a copper/constantan thermocouple.

The fitted polynomial is as follows:

$$\Delta V(T) = 4.08 * 10^{-8} * T^2 + 1.64 * 10^{-5} * T - 8.39 * 10^{-3} \tag{3.1}$$

Afterwards, the scattering and the correlation coefficient R^2 were computed to determine the quality of the fit. The scattering, which is the fitted function subtracted by the measured data, can be seen in figure 3.6. The exact value of the correlation coefficient turned out to be $R^2 = 0.9999999961871723$. The closer it is to unity, the better the quality of the fit, which means that equation (3.1) is an excellent fit for our data.
As can be seen in figure 3.6, the scattering negligibly small. Correspondingly, the root mean square error is also negligibly small as $\sigma_{rms} = 9.33 * 10^{-8}$.

Solving equation (3.1) for the temperature, yields us the necessary expression for the conversion from voltage to temperature:

$$T(\Delta V) = \frac{-1.64 * 10^{-5} + \sqrt{2.69 * 10^{-10} + 1.63 * 10^{-7}(\Delta V + 8.39 * 10^{-3})}}{8.16 * 10^{-8}} \tag{3.2}$$

where we only restrict ourselves to positive values of $T(\Delta V)$ as there are no negative temperature values.

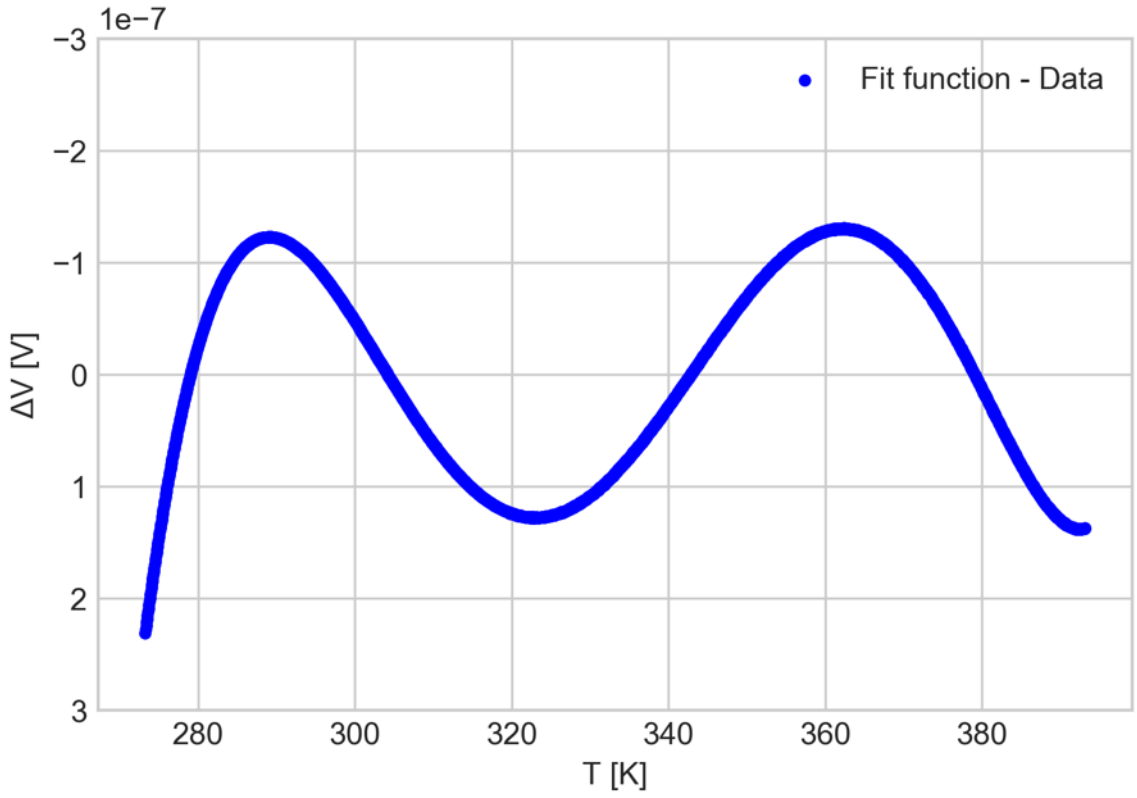

Figure 3.6: Difference of the fitted function (equation (3.1)) and the measured data from the table.

3.3 Testing

The next step is to test the experiment. The less scattering we have, the more accurate the result will be, so different methods of thermal insulation for the experiment have to be tested. This is also important because we are neglecting any thermal radiation in section 2.2. In each of the tests, I used a soldering iron to create a ΔT of roughly $12K$. The first test was without any thermal insulation, the results can be seen in figure 3.7.

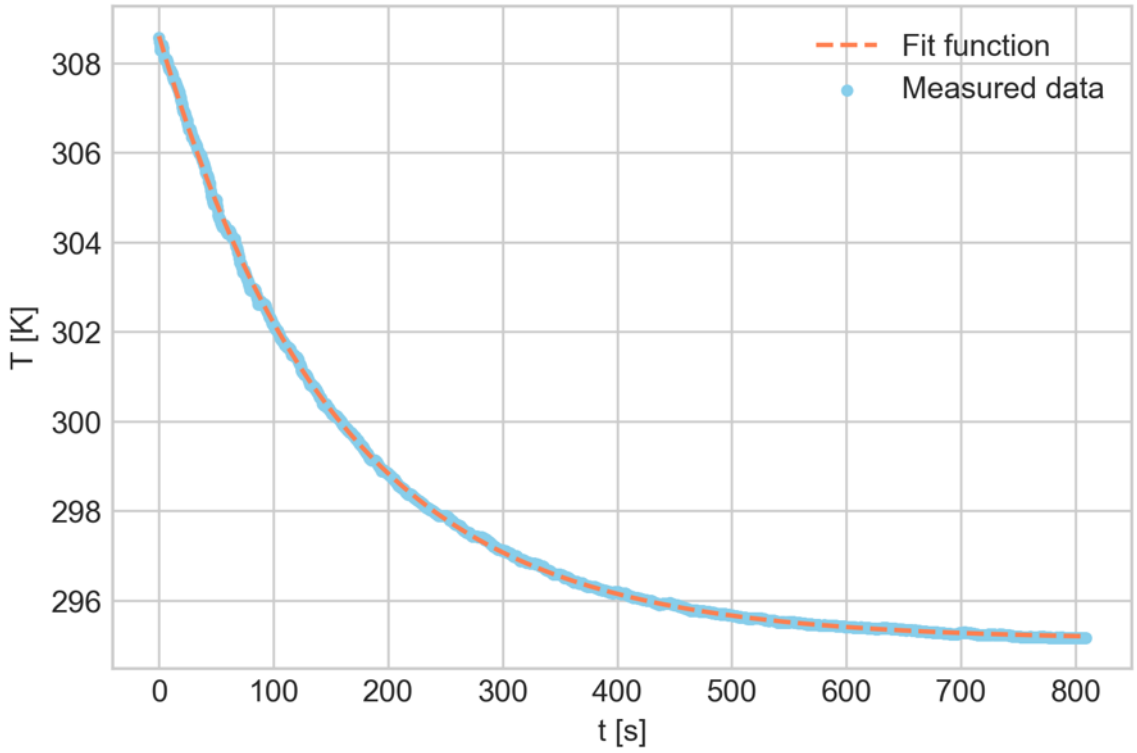

(a) $T_H(t)$ data and fit of the process of cooling down

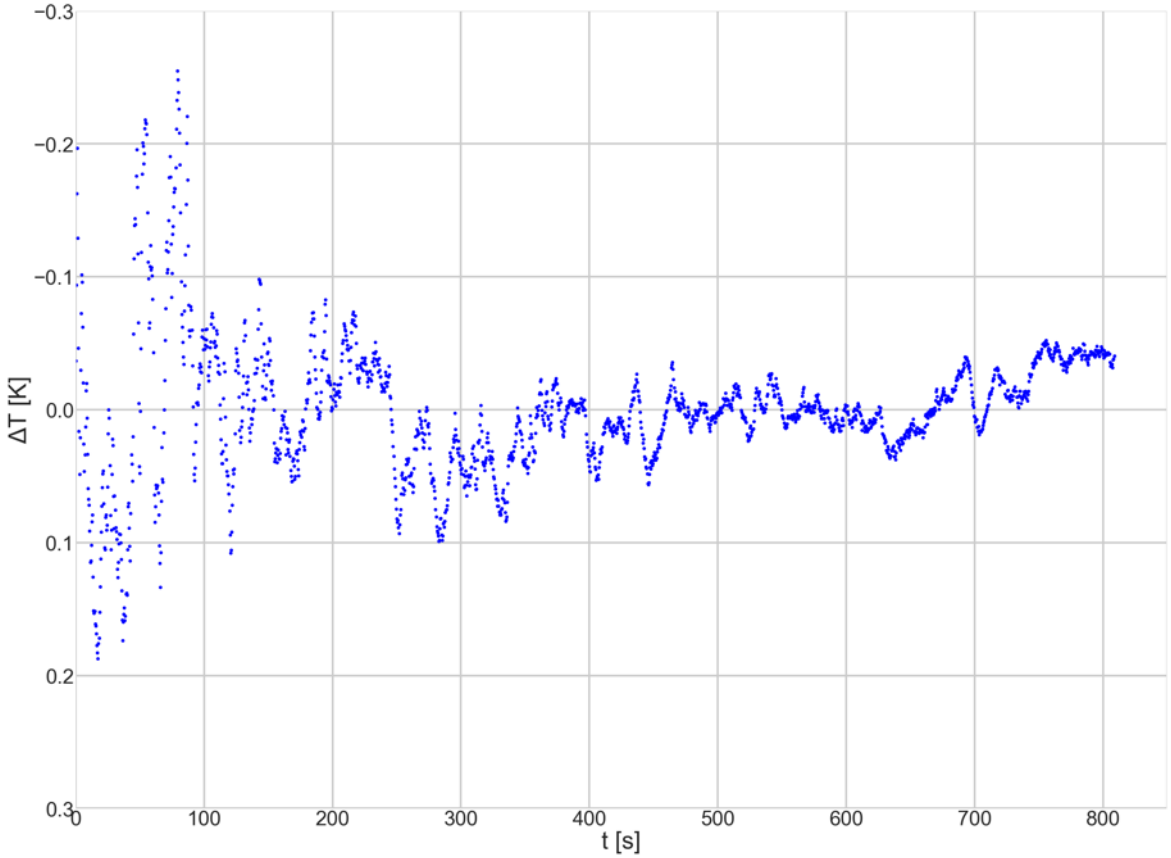

(b) Scattering obtained by subtracting the measured data by the fit in (a).

Figure 3.7: Test 1: No thermal insulation

As can be seen, the scattering in figure 3.5 (b) is quite large, especially when compared to the tests where thermal insulation has been used. In fact, the scattering can even be seen from the exponential fit in figure 3.5 (a). Only the process of cooling down has been considered here, since it is not practical to use the process of heating up while a soldering iron was used.

The second test was run by using a glass container to cover up the experiment. The result of this test can be seen in figure 3.8.

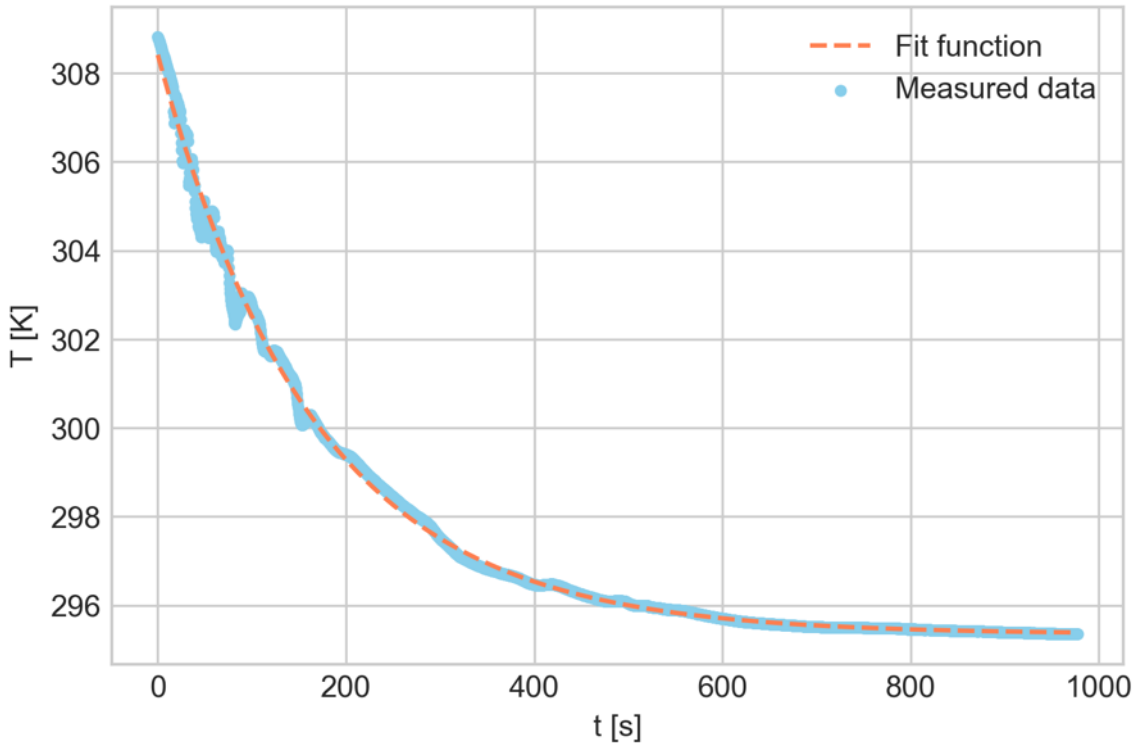

(a) $T_H(t)$ data and fit of the process of cooling down

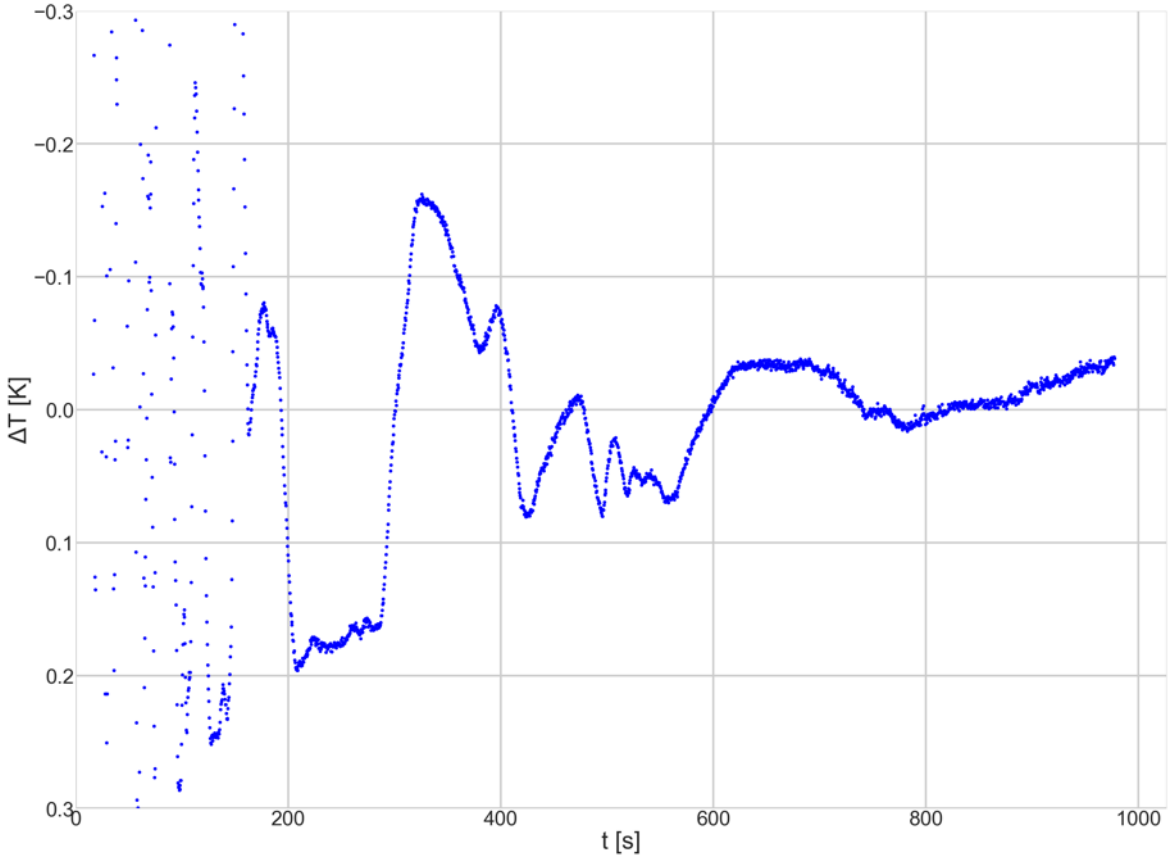

(b) Scattering obtained by subtracting the measured data by the fit function in (a).

Figure 3.8: Test 2: Glass container over experiment

The scattering in this case is even more extreme than without any thermal insulation. The reason behind this is that a window was opened in the room where the experiment was conducted during the measurement. However, this is conclusive that a glass container covering the experiment is not suitable for thermal insulation.

The next test involved a piece of cloth covering the experiment. My sweater served as a piece of cloth in this test. The result can be seen in figure 3.9.

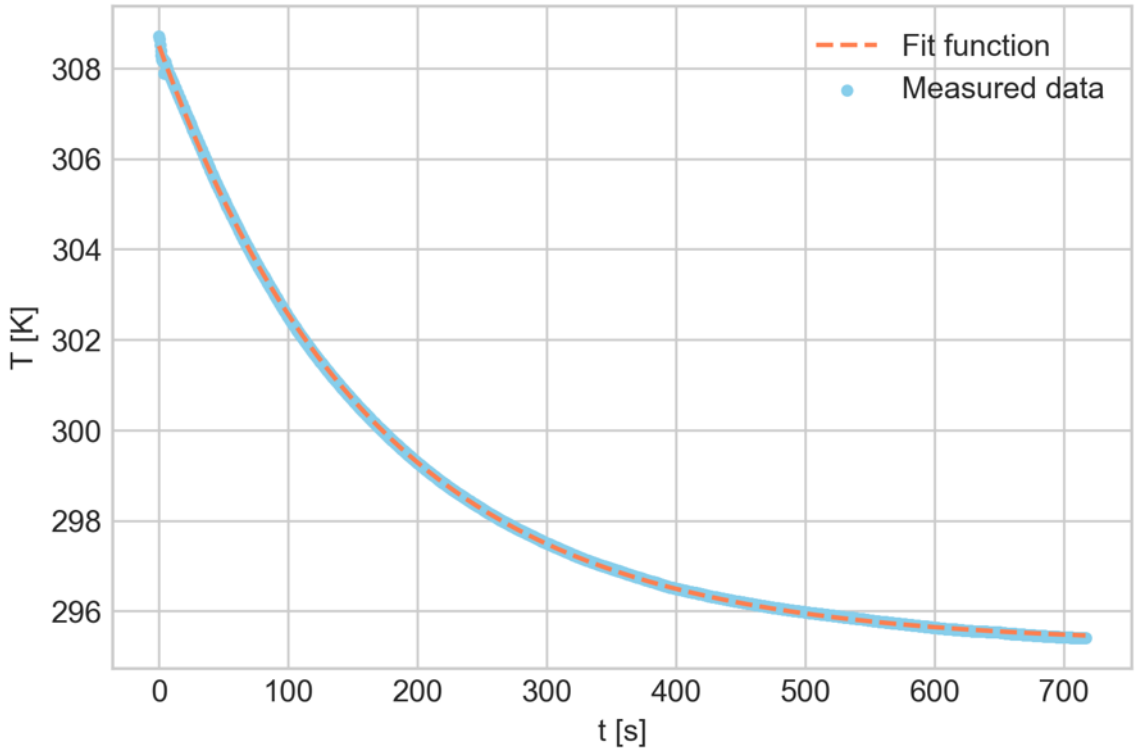

(a) $T_H(t)$ data and fit of the process of cooling down

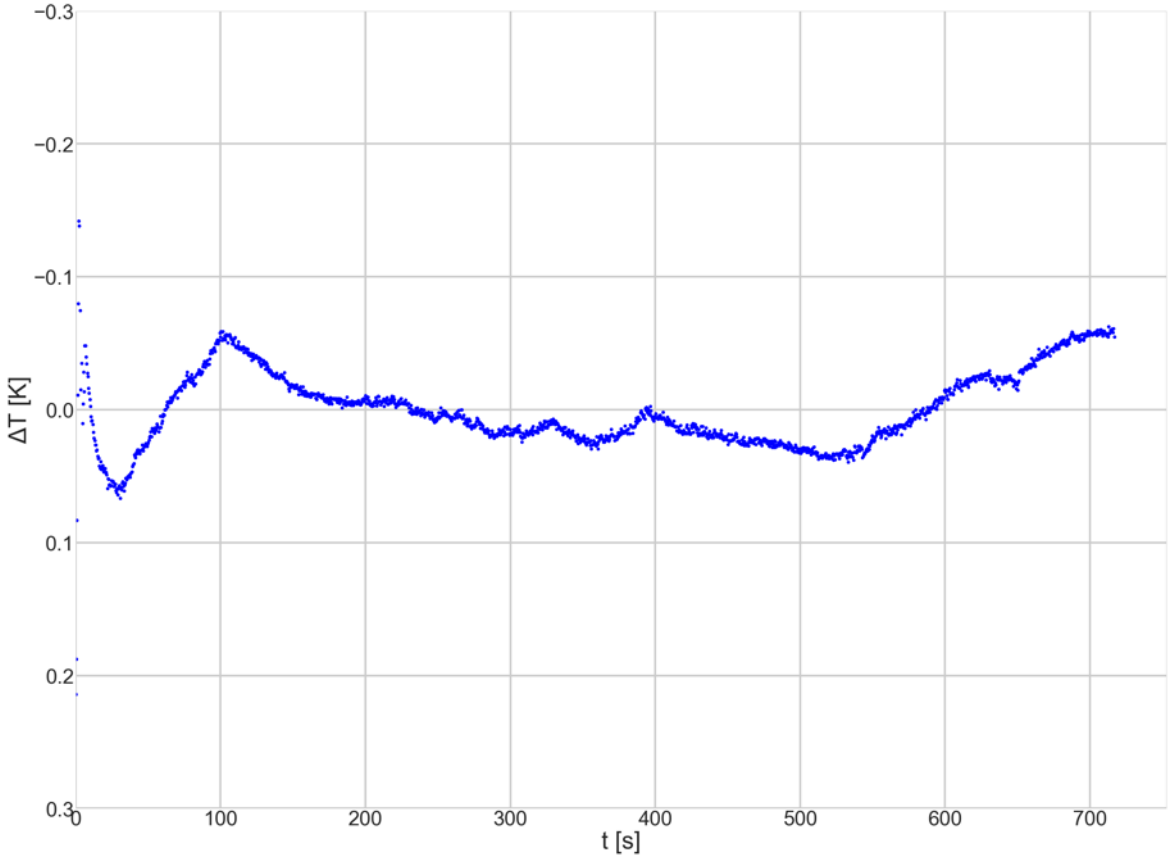

(b) Scattering obtained by subtracting the measured data by the fit function in (a).

Figure 3.9: Test 3: Cloth over experiment

This time, the scattering is on a much smaller scale than before. There was no noticeable difference between the scattering when the window was closed and when it was opened.

The fourth test involved covering the experiment in a container of Styrofoam. For this, a suitable body of Styrofoam was cut into shape such that it could cover the experiment without any gaps. However, as can be seen in figure 3.4, the Styrofoam container was quite tall. Since it is hollow, it means that there still is a considerable amount of air inside. The results of this test can be seen in figure 3.11.

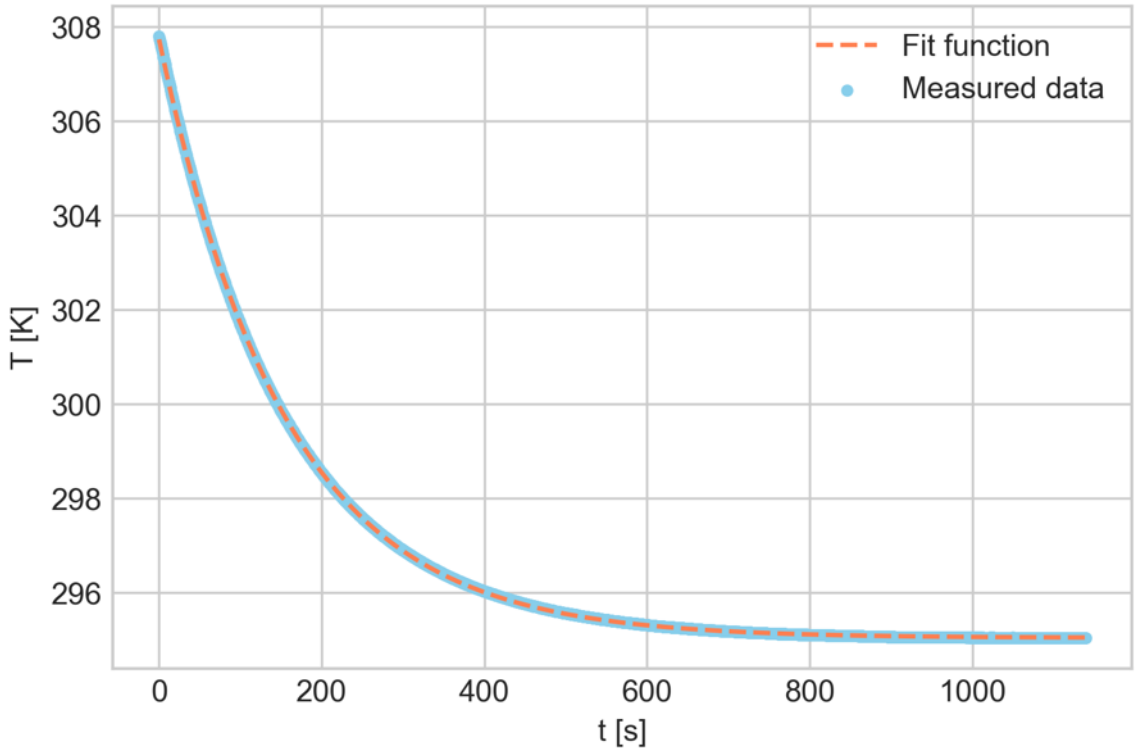

(a) $T_H(t)$ data and fit of the process of cooling down

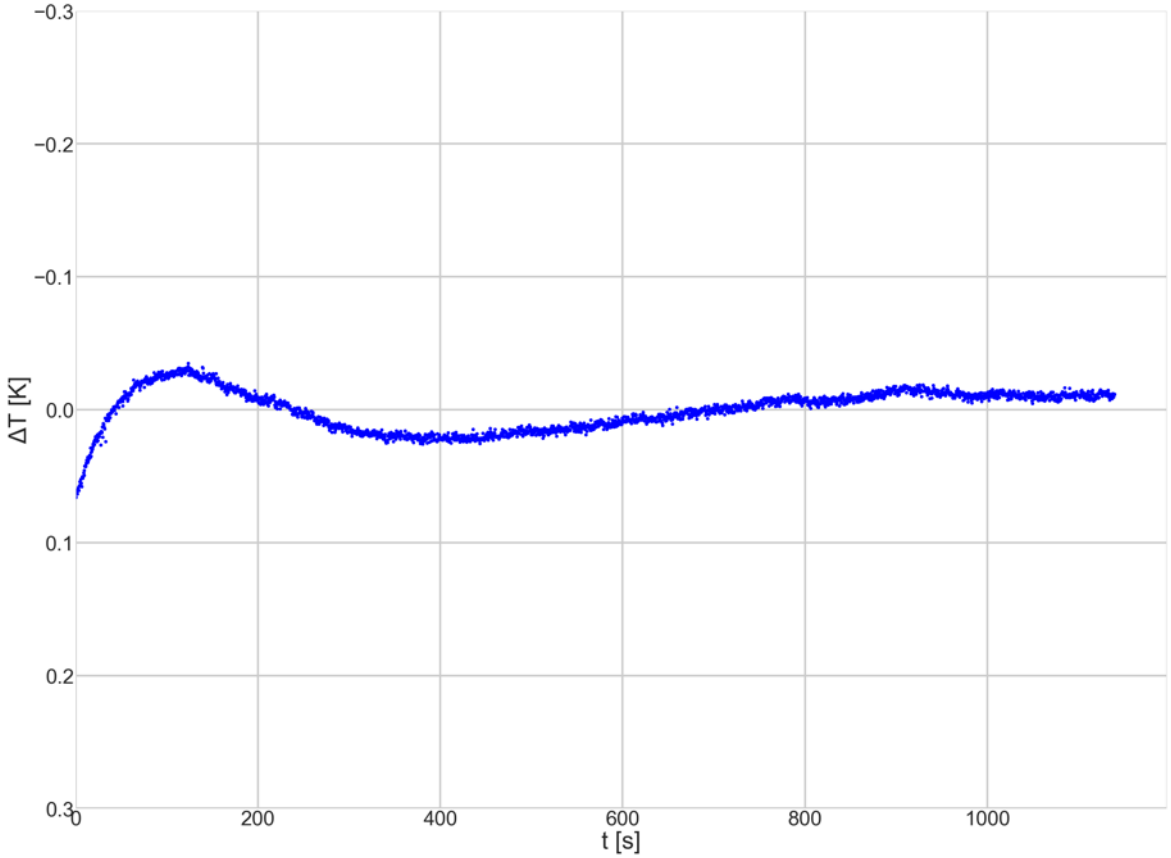

(b) Scattering obtained by subtracting the measured data by the fit function in (a).

Figure 3.10: Test 4: Styrofoam over experiment

The result is more satisfactory than the result where cloth was used. The scattering is smaller and more even.

In the final test, the hollow body of the Styrofoam container was filled with paper, commonly used to dry hands. The results of this can be seen in figure 3.9.

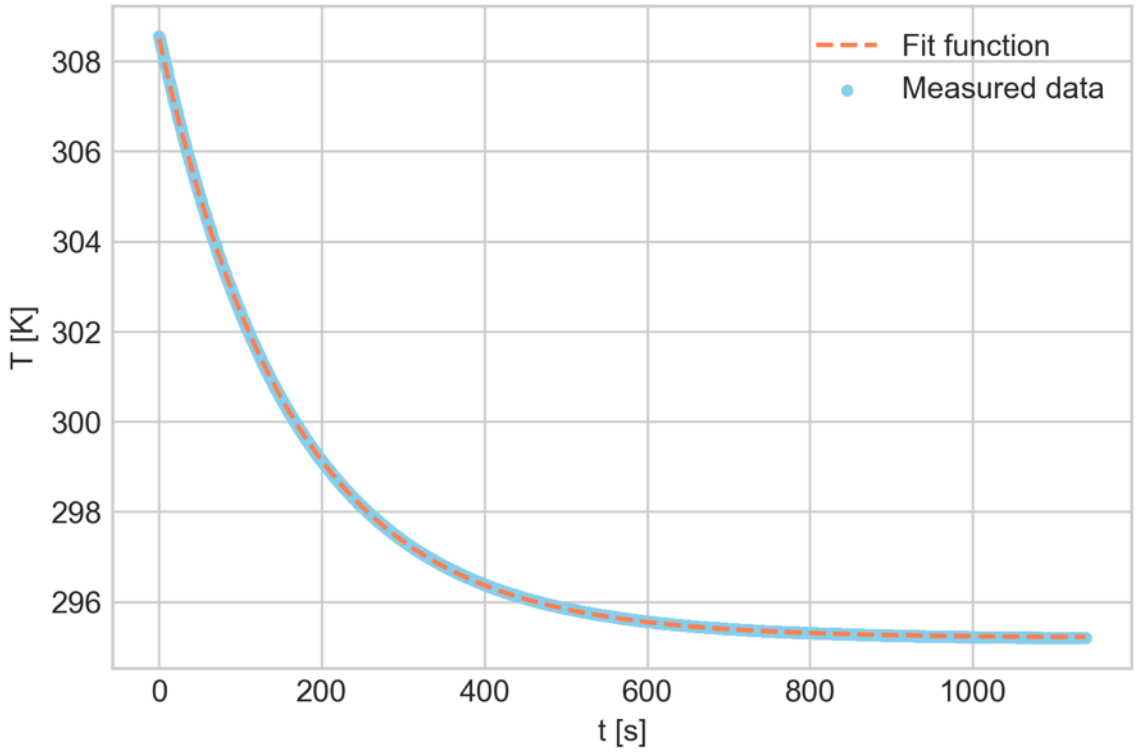

(a) $T_H(t)$ data and fit of the process of cooling down

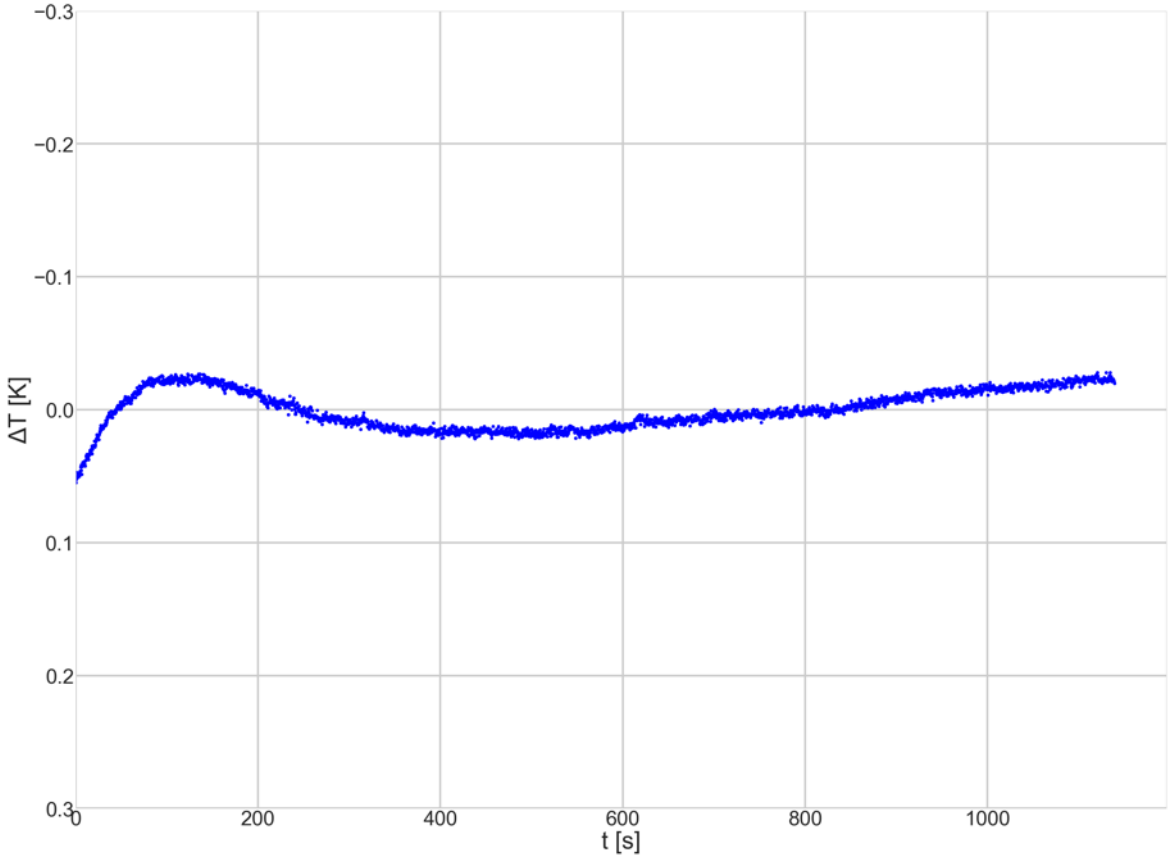

(b) Scattering obtained by subtracting the measured data by the fit function in (a).

Figure 3.11: Test 5: Styrofoam with paper over experiment

This is the best result as it has the smallest scattering. Nevertheless, the actual measurements have been done for both cases, with and without paper inside the Styrofoam container.

3.4 Measurements

I began taking measurements for the determination of ZT as soon as the heater was successfully attached onto the small copper body. My measuring methodology went as follows:

First, I would use a different electrical resistance which has the same value as the heater ($R_H = 10\Omega$) in order to prepare the power supply to drive a given current through the heater to achieve a predetermined temperature gradient ΔT. The currents for which I aimed for, the corresponding voltage of the power supply and the resulting heating power can be seen in table 3.1 below.

$\Delta T[K]$	$P_H[W]$	$V[V]$	$I[A]$
10	0.317	1.78	0.178
20	0.636	2.52	0.252
30	0.954	3.09	0.309
40	1.272	3.57	0.357
50	1.590	3.99	0.399
60	1.908	4.37	0.437
70	2.228	4.72	0.472
80	2.540	5.04	0.504

Table 3.1: Temperature gradients which were aimed for in the experiment.

The needed current for a predetermined ΔT was obtained through equation (2.46), where $\dot{Q} = P_H$ and only positive values of $\Delta T = \frac{P_H}{k}$ were considered. The required value of the thermal conductivity k was obtained through an article by Prof. Dr. Schilling in which he used the same experiment. Its value has been taken as $k = 0.0318W/K$ [10]. The current which is to be set up at the power supply is then given by:

$$P_H = I^2 R_H \tag{3.3}$$

$$I = \sqrt{P_H/R_H} \tag{3.4}$$

Finally, the voltage is obtained by simply applying $V = R_H I$. It should be noted that table 3.1 only serves as a rough reference. Setting up a current at the power supply was a very inaccurate process. However, this did not matter because ΔT was obtained from the fit function according to equation (2.29) anyways.

After setting up a current, I plugged in the heater into the power supply, the power supply being turned off. I would then start the data logging and leave it running for one minute until I would turn on the power supply which started the heating process. I would let it heat for 20 minutes and then turn the power supply off again, initiating the process of cooling down. The data would log for 20 more minutes until stopping. An example of a raw measurement following this methodology can be seen in figure 3.12.

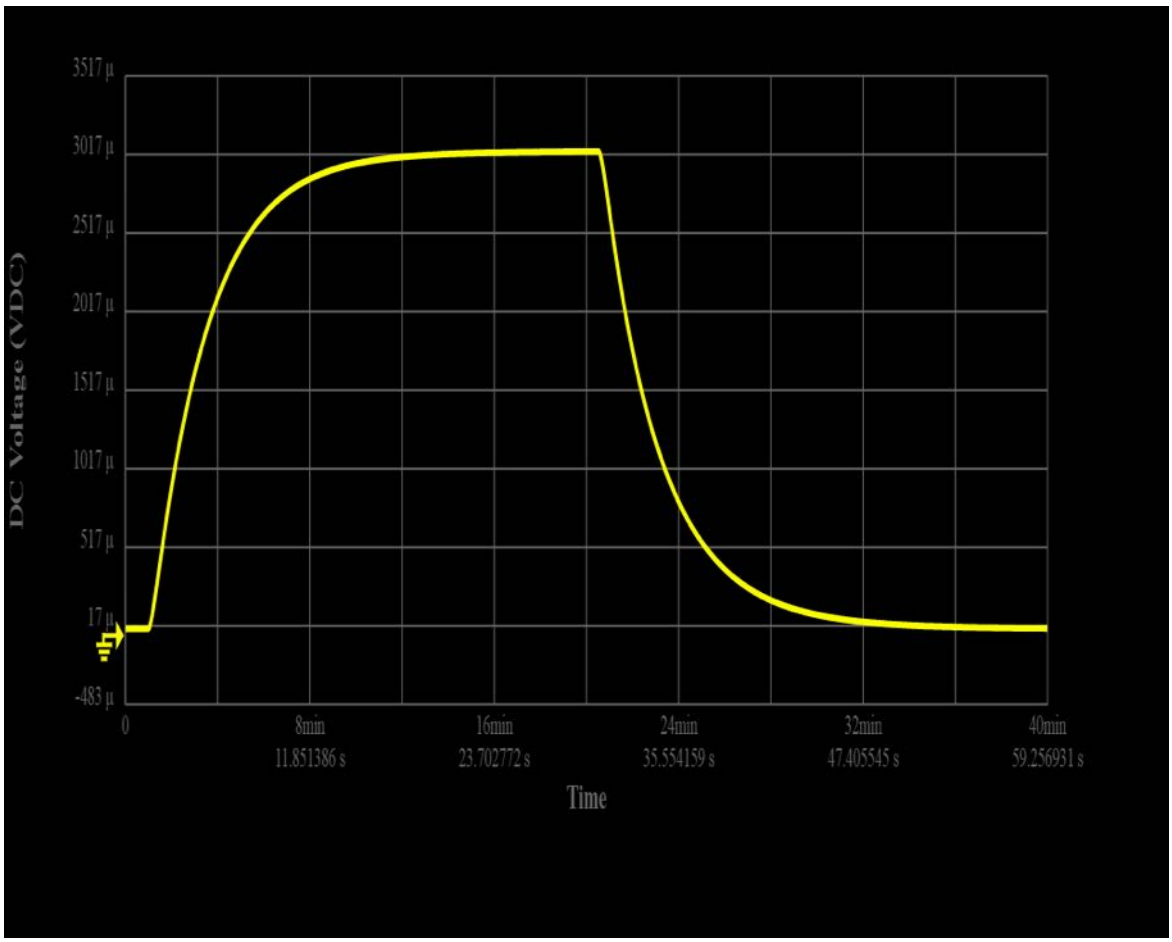

Figure 3.12: Raw measurement data as seen directly from the data logging software. The first minute of the measurement is with the power supply off. The next 20 minutes are with the power supply on, afterwards another 20 minutes of cooling with the power supply off are measured.

As expected in section 2.1, the process of heating up and cooling down seem to be an exponential growth and decay correspondingly.
Afterwards, I would export the raw data as a csv file and separate the processes of heating up and cooling down by hand. For the process of cooling down, I kept two versions. One version included the entire process, right from the moment where the power supply was turned off. In the other version, I would prune the data such that the first 60 seconds of the process are not included. The reason for this was that the heater still carries some heat after the power supply is turned off. If I included this data, I would get a different fit function because of this lingering heat source, so I decided to wait in order to only include the cooling down of the small copper body, and not the heater itself as well.
Nothing was done with the first minute of the measurement. This only served as a way to compare ΔT with the temperature gradient of the fit, in case anything went wrong.
In total, 24 measurements were done. Two sets of measurements according to table 3.1 with paper inside the Styrofoam container and one set of measurements without paper.
With this data, it was possible to determine ZT according to sections 2.1 and 2.2. All data analysis was done in python. The method used to find fit functions was the method of least squares.

In order to compare the ZT obtained via the new method to the ZT obtained using the standard method, measuring α, R_{TE} and k separately was required as well. The measurements of α and k could be done by adding one additional apparatus to the experimental setup, namely a second volt meter according to figure 3.4.
The Seebeck coefficient α was determined by measuring the Seebeck voltage across the thermoelectric cooler. Using equation (1.1), we get:

$$\alpha = \frac{\Delta V_S}{\Delta T} \tag{3.5}$$

where ΔT was obtained via the fit function during the process of heating up.
The thermal conductivity k was obtained using equation (2.46). Solving for k and using $\dot{Q} = P_H$, we get:

$$k = \frac{P_H}{\Delta T} \tag{3.6}$$

$$k = \frac{I^2 R_H}{\Delta T} \tag{3.7}$$

where I was the current driven through the heater. Since the power supply did not have a sufficiently accurate display to show the current, the voltage across the heater R_H was measured and the exact current I was determined through $I = V/R_H$.
The circuit diagram for the determination of α and k can be seen in figure 3.13.

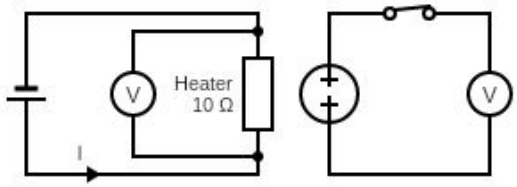

Figure 3.13: Circuit diagram for the determination of α and k. The DC voltage source on the right part of the diagram represents the inactive thermoelectric cooler which generates a DC voltage due to the Seebeck effect.

The determination of the internal resistance of the thermoelectric cooler R_{TE} was more involved than this due to the appearance of a "false" resistance as described in section 2.3.
One of the simplest and most precise methods to measure R_{TE} is the so-called instant load-voltage analysis method. It requires an additional load resistance R_{Load} as seen in figure 3.4. In this case, the load resistance was
$R_{Load} = 1\Omega$.
The Seebeck voltage, once the small copper body is heated up to T_H with an open circuit, is again given by equation (1.1) and according to Ohm's law we get:

$$\Delta V_S = \alpha \Delta T \tag{3.8}$$

$$\Delta V_S = I(R_{TE} + R_{Load}) =: V_{M1} \tag{3.9}$$

V_{M1} is the same voltage measured, which is used for determining α. Solving for R_{TE}, the following expression is obtained:

$$R_{TE} = \frac{V_{M1} - I R_{Load}}{I} \tag{3.10}$$

When the circuit is now closed and the load resistance is connected in series with the thermoelectric cooler, a current I will flow through the thermoelectric cooler due to the Seebeck voltage. This current then leads to the Peltier effect which causes the small copper body to cool down, lowering the value of ΔT. If this temperature change is corrected back to what it was in the open circuit by increasing the current being driven through the heater by the power supply, we can measure another voltage V_{M2} across the load resistance. We need to correct ΔT due to the fact that we expressed V_{M1} in terms of R_{Load} instead of R_{TE} only. Compared to V_{M1}, the load resistance causes a voltage drop through the circuit. V_{M2} thus is the sum of the voltage drops:

$$V_{M2} = V_{M1} - IR_{TE} = IR_{Load} \tag{3.11}$$

Using the expression of IR_{Load} from equation (3.11) and applying it in equation (3.10), we can express the internal resistance of the thermoelectric cooler as follows [19]:

$$R_{TE} = \frac{V_{M1} - V_{M2}}{I} \tag{3.12}$$

Using the fact that $I = V_{M2}/R_{Load}$, we arrive to the following expression for R_{TE}:

$$R_{TE} = \left(\frac{V_{M1}}{V_{M2}} - 1\right) R_{Load} \tag{3.13}$$

The setups for measuring V_{M1} and V_{M2} can be seen in figure 3.15.

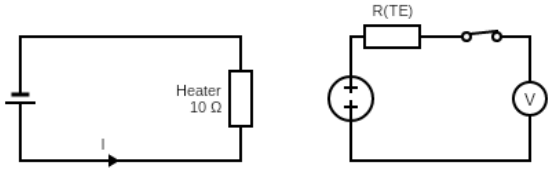

(a) Measurement of V_{M1}. This is the same process as the measurement of α.

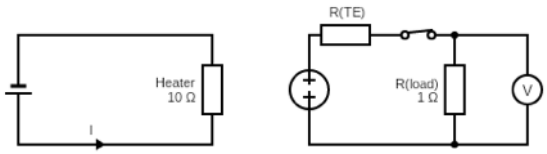

(b) Measurement of V_{M2}. A current I now flows through the circuit and the voltage drop is measured across the load resistance.

Figure 3.14: Circuit diagrams for measuring V_{M1} and V_{M2}.

However, up until now, we have completely neglected the resistance of the cables through which the current flows as well. Since this is now included in our R_{TE}, we can simply measure the resistance of the cables R_C using the four-point probes method and subtract it from R_{TE}. The resistance of the cables turned out to be $R_C = 0.036\Omega$. We arrive at our final expression for the internal resistance of the thermoelectric cooler:

$$R'_{TE} = R_{TE} - R_C \tag{3.14}$$

Results and Analysis

4.1 Determination of ZT using the first method

The first method for the determination of ZT involves fitting a function described by equation (2.34) during the process of heating up and equations (2.11) and (2.29) during the process of cooling down through the measured data points. Summarizing equations (2.11) and (2.29), we get:

$$T_H(t) = \Delta T exp\left(-\frac{t}{\tau_{1,2}}\right) + T_C \tag{4.1}$$

We can then extract τ_1 and τ_2 from the fit function and determine ZT using equation (2.33). I ran two sets of measurements with paper inside the Styrofoam container. The results of the first set of measurements can be seen in table 4.1 below.

N	I[A]	$\Delta T[K]$	Circuit	τ heating [s]	τ cooling [s]
1.0	0.19	11.38±0.01	open	153.18±0.14	163.97±0.03
1.0	0.19	8.46±0.01	closed	113.66±0.1	119.02±0.04
2.0	0.25	18.85±0.1	open	153.34±0.08	164.10±0.03
2.0	0.25	14.16±0.01	closed	113.31±0.1	118.29±0.03
3.0	0.31	29.77±0.01	open	151.98±0.09	162.86±0.04
3.0	0.31	22.86±0.01	closed	112.30±0.1	118.13±0.03
4.0	0.34	36.28±0.01	open	151.32±0.1	163.22±0.04
4.0	0.34	26.87±0.01	closed	111.67±0.09	117.98±0.03
5.0	0.38	44.97±0.02	open	151.92±0.12	163.40±0.05
5.0	0.38	33.05±0.02	closed	111.50±0.1	117.97±0.04
6.0	0.42	54.28±0.02	open	151.53±0.12	164.40±0.03
6.0	0.42	40.10±0.02	closed	111.52±0.1	117.39±0.03
7.0	0.47	63.56±0.02	open	150.09±0.09	162.00±0.04
7.0	0.47	47.89±0.03	closed	110.75±0.1	117.14±0.03
8.0	0.50	72.69±0.03	open	146.49±0.09	161.62±0.04
8.0	0.50	54.70±0.03	closed	109.84±0.1	116.81±0.03

Table 4.1: Results of the first set of measurements with paper inside the Styrofoam container. N denotes the measurement number and I the current driven through the heater. "Circuit open" means the thermoelectric cooler is inactive and we measure τ_1 while "Circuit closed" means the thermoelectric cooler is active and we measure τ_2.

As can be seen, the higher the temperature gradient ΔT, the lower $\tau_{1,2}$ seem to be, indicating a first temperature dependence of $\tau_{1,2}$. It can also clearly be seen that $\tau_2 < \tau_1$, which makes sense considering the small copper body should cool down more quickly when the thermoelectric cooler is cooling.
Another indication that $\tau_{1,2}$ depend on temperature is the fact that τ heating and τ cooling do not share the same values, as mentioned in section 2.1.

An example of a fit can be seen in figure 4.1. The uncertainties on ΔT and τ were obtained by taking the square root of the corresponding diagonal entry on the covariant matrix [20]. In all of the fits used to obtain the data in table 4.1, the value of the correlation coefficient R^2 is above 0.999, indicating a good quality of the fits.

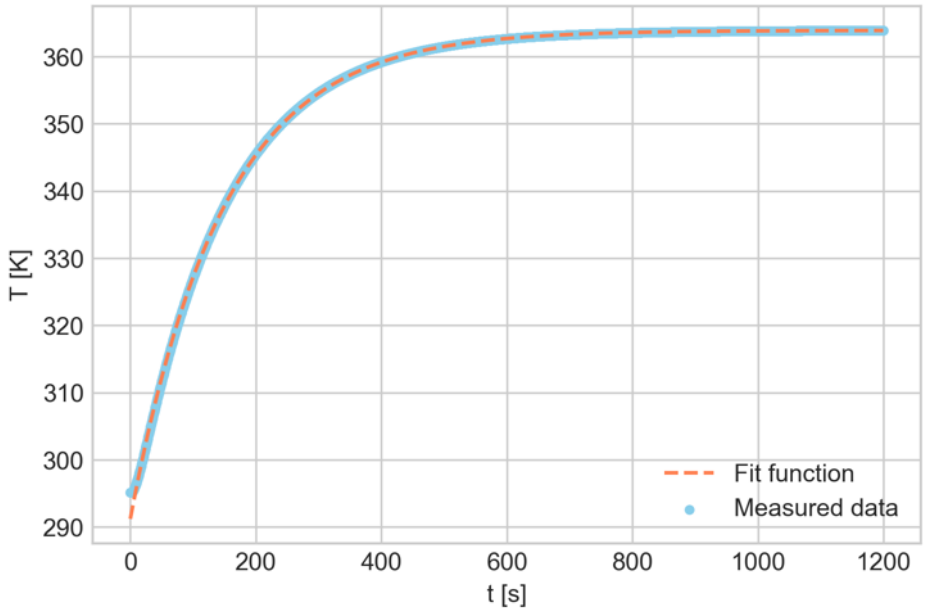

(a) Fit of the data during heating.

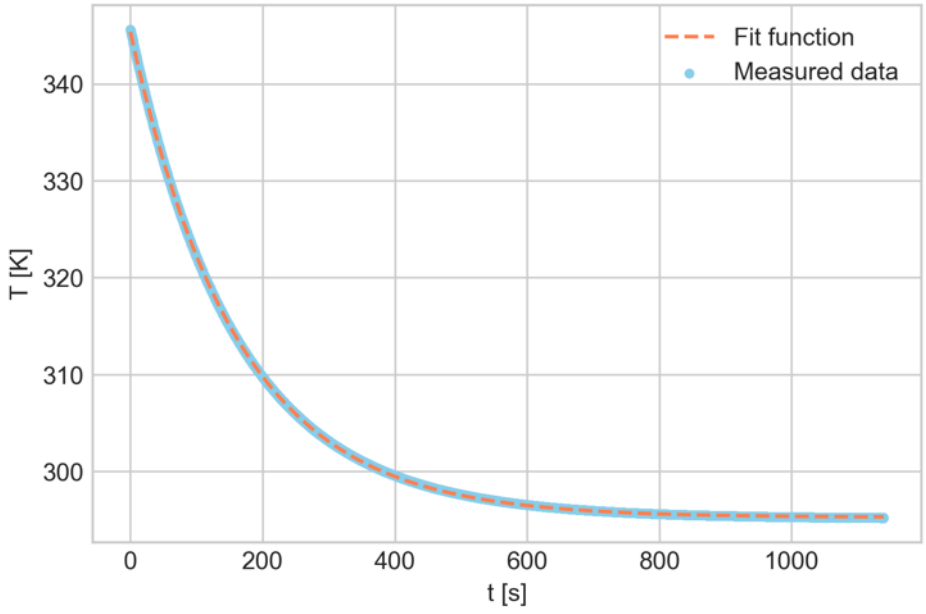

(b) Fit of the data during cooling.

Figure 4.1: An example of fit functions of the measured data. In this case, the fits correspond to measurement 8.0 with an open circuit.

The resulting figures of merit ZT can be seen in table 4.2.

N	$T_{avg}[K]$	ZT cooling	ZT heating
1.0	299.19±0.01	0.378	0.348
2.0	301.93±0.1	0.387	0.353
3.0	305.95±0.01	0.379	0.353
4.0	308.35±0.01	0.383	0.355
5.0	311.54±0.02	0.385	0.363
6.0	314.97±0.02	0.400	0.359
7.0	318.38±0.02	0.383	0.355
8.0	321.74±0.03	0.384	0.334

Table 4.2: Results of ZT obtained through the measurements described in table 4.1 using equation (2.33).

The temperature T_{avg} was obtained from the fact that these values of ZT are averaged over the temperature range of the exponential fit. Its value was computed using $T_{avg} = T_C + \Delta T/e$ and the uncertainty of ZT was computed using the error propagation law for standard deviations, however, it was too small to include. As can be seen, no convincing temperature dependence can be seen from table 4.2, which might imply that this method of determining ZT is only good for a rough estimation of the figure of merit. Fitting a regression line through the data seen in table 4.2 in order to try and determine a temperature dependence of ZT yields a very poor quality fit, hence it is not worth showing here.

If we naively assume that ZT is thus temperature independent, we can compute the mean:

$$ZT_C = 0.385 \pm 0.006 \tag{4.2}$$

$$ZT_H = 0.353 \pm 0.008 \tag{4.3}$$

where the uncertainty is the standard deviation.

The second set of measurements with paper inside the Styrofoam container gave results seen in table 4.3.

N	I[A]	$\Delta T[K]$	Circuit	τ heating [s]	τ cooling [s]
1.1	0.19	11.51±0.01	open	153.09±0.08	163.97±0.03
1.1	0.19	8.53±0.01	closed	115.34±0.1	118.02±0.03
2.1	0.25	20.10±0.1	open	154.56±0.08	163.95±0.03
2.1	0.25	15.24±0.01	closed	113.80±0.1	118.00±0.03
3.1	0.31	28.84±0.01	open	154.05±0.08	163.09±0.03
3.1	0.31	21.46±0.01	closed	111.95±0.09	117.30±0.03
4.1	0.34	37.59±0.01	open	152.73±0.09	163.00±0.04
4.1	0.34	28.09±0.02	closed	110.80±0.1	117.36±0.03
5.1	0.38	44.58±0.01	open	151.52±0.08	162.29±0.03
5.1	0.38	33.38±0.02	closed	111.07±0.1	117.25±0.03
6.1	0.42	52.93±0.02	open	149.86±0.09	161.97±0.04
6.1	0.42	39.42±0.02	closed	110.33±0.09	117.00±0.03
7.1	0.47	69.18±0.02	open	147.47±0.09	161.75±0.04
7.1	0.47	51.84±0.03	closed	109.83±0.09	117.12±0.04
8.1	0.50	73.67±0.02	open	145.68±0.08	161.38±0.04
8.1	0.50	55.39±0.03	closed	108.73±0.08	116.67±0.03

Table 4.3: Results of the second set of measurements, denoted with .1 after the measurement number, with paper inside the Styrofoam container.

The resulting figures of merit ZT can be seen in table 4.4.

N	$T_{avg}[K]$	ZT cooling	ZT heating
1.1	299.23±0.01	0.389	0.327
2.1	302.39±0.1	0.389	0.358
3.1	305.61±0.01	0.390	0.377
4.1	308.83±0.01	0.398	0.378
5.1	311.40±0.01	0.384	0.364
6.1	314.47±0.02	0.384	0.358
7.1	320.45±0.02	0.381	0.343
8.1	322.10±0.02	0.383	0.340

Table 4.4: Results of ZT obtained through the measurements described in table 4.1 using equation (2.33).

A resemblance of a temperature dependence can be seen here for ZT (cooling), especially if measurement 4.1 is ignored. There seems to be a slight downtrend for ZT (cooling) as the temperature rises.
If we now additionally fit a regression line through the data seen in table 4.4, we get an expression for the temperature dependence of ZT. Only ZT (cooling) has been considered here and the result can be seen in figure 4.2.
The resulting fit function is as follows:

$$ZT = -5.264 * 10^{-4} * T + 0.551 \tag{4.4}$$

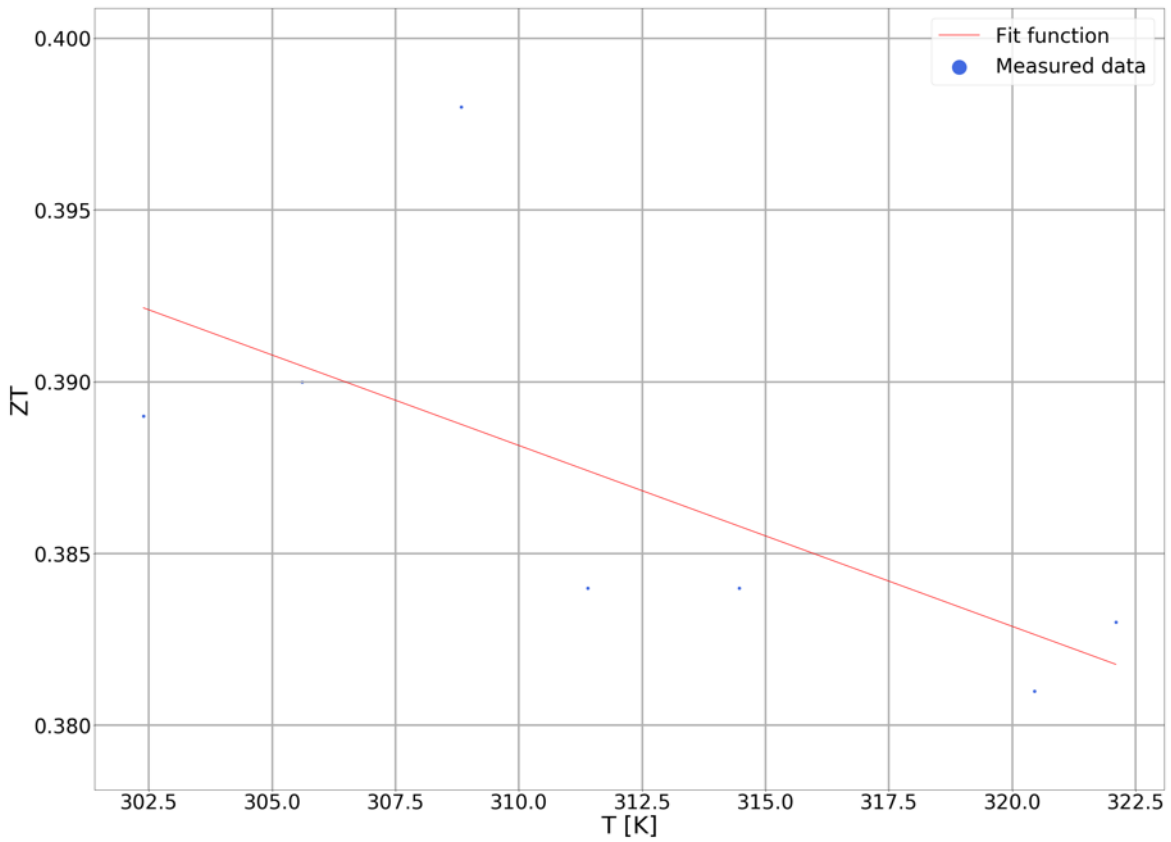

Figure 4.2: Fit function of ZT (cooling) with the data obtained from table 4.4. The uncertainties on the data points are too small to be shown.

Expressing ZT analogue to equations (4.2) and (4.3), we get:

$$ZT_C = 0.387 \pm 0.005 \tag{4.5}$$

$$ZT_H = 0.356 \pm 0.017 \tag{4.6}$$

Equations (4.5) and (4.6) seem to be compatible with (4.2) and (4.3), showing good reproducibility of the experiment. However, the fact that $ZT_C \neq ZT_H$ is reason enough to believe that ZT is dependent on temperature.

The results for the measurement set where there was no paper inside the Styrofoam container should be different from the results mentioned above, considering the thermal insulation is different. They can be seen in table 4.5.

N	I[A]	$\Delta T[K]$	Circuit	τ heating [s]	τ cooling [s]
1.2	0.19	11.24±0.01	open	146.16±0.08	157.79±0.03
1.2	0.19	8.49±0.01	closed	107.13±0.09	113.78±0.02
2.2	0.25	18.69±0.01	open	144.15±0.08	155.49±0.03
2.2	0.25	14.07±0.01	closed	105.91±0.09	112.51±0.02
3.2	0.31	27.91±0.01	open	141.97±0.08	154.61±0.04
3.2	0.31	21.05±0.01	closed	105.53±0.09	112.61±0.02
4.2	0.34	32.67±0.01	open	140.44±0.08	153.95±0.04
4.2	0.34	24.28±0.01	closed	104.36±0.09	112.23±0.02
5.2	0.38	40.68±0.01	open	139.17±0.08	153.25±0.04
5.2	0.38	30.82±0.02	closed	103.43±0.09	112.06±0.02
6.2	0.42	48.73±0.02	open	138.24±0.08	152.49±0.04
6.2	0.42	37.12±0.02	closed	103.33±0.1	111.39±0.02
7.2	0.47	58.73±0.02	open	136.13±0.08	151.83±0.04
7.2	0.47	44.84±0.02	closed	102.27±0.09	111.19±0.03
8.2	0.50	67.72±0.03	open	133.59±0.09	151.28±0.04
8.2	0.50	51.57±0.03	closed	101.80±0.08	111.03±0.02

Table 4.5: Results of the second set of measurements without paper inside the Styrofoam container, denoted with .2 after the measurement number.

It can immediately be seen that compared to the results where there was paper inside the Styrofoam container (tables 4.1 and 4.3), the temperature gradients ΔT seem to be smaller if there is no paper used. This is concluding evidence that there is considerably less thermal insulation if there is no paper inside the Styrofoam container. The time constants τ are smaller as well, sharing the similarity with the case before that the higher the temperature gradient, the smaller the time constant. What is also noticeable is the fact that the higher the temperature gradient ΔT, the more the values of the time constants differ from the measurement sets with paper inside the Styrofoam container. This could imply that the case where there is no paper used might only be accurate for small temperature gradients.

The corresponding values of figures of merit ZT can be seen in table 4.6

N	$T_{avg}[K]$	ZT cooling	ZT heating
1.2	299.13±0.01	0.388	0.364
2.2	301.88±0.01	0.382	0.361
3.2	305.27±0.01	0.373	0.345
4.2	307.02±0.01	0.372	0.346
5.2	309.67±0.01	0.368	0.346
6.2	312.93±0.02	0.369	0.338
7.2	316.61±0.02	0.367	0.331
8.2	319.95±0.03	0.363	0.312

Table 4.6: Results of ZT obtained through the measurements described in table 4.1 using equation (2.33).

A clear decrease of ZT can be seen as the temperature rises, however, this is most likely due to the fact that there is less thermal insulation than before. The loss of heat is proportional to ΔT after all. The fact that ZT from measurement number 1.2 is inside the error of margin of equations (4.5) and (4.2) supports the earlier statement that this method could be used to estimate ZT for small temperature gradients. If

we fit a regression line using the data from table 4.6 to determine the temperature dependence of ZT (cooling) anyways, we obtain the following equation:

$$ZT = -8.553 * 10^{-4} * T + 0.636 \tag{4.7}$$

The graphical result can be seen in figure 4.3 below.

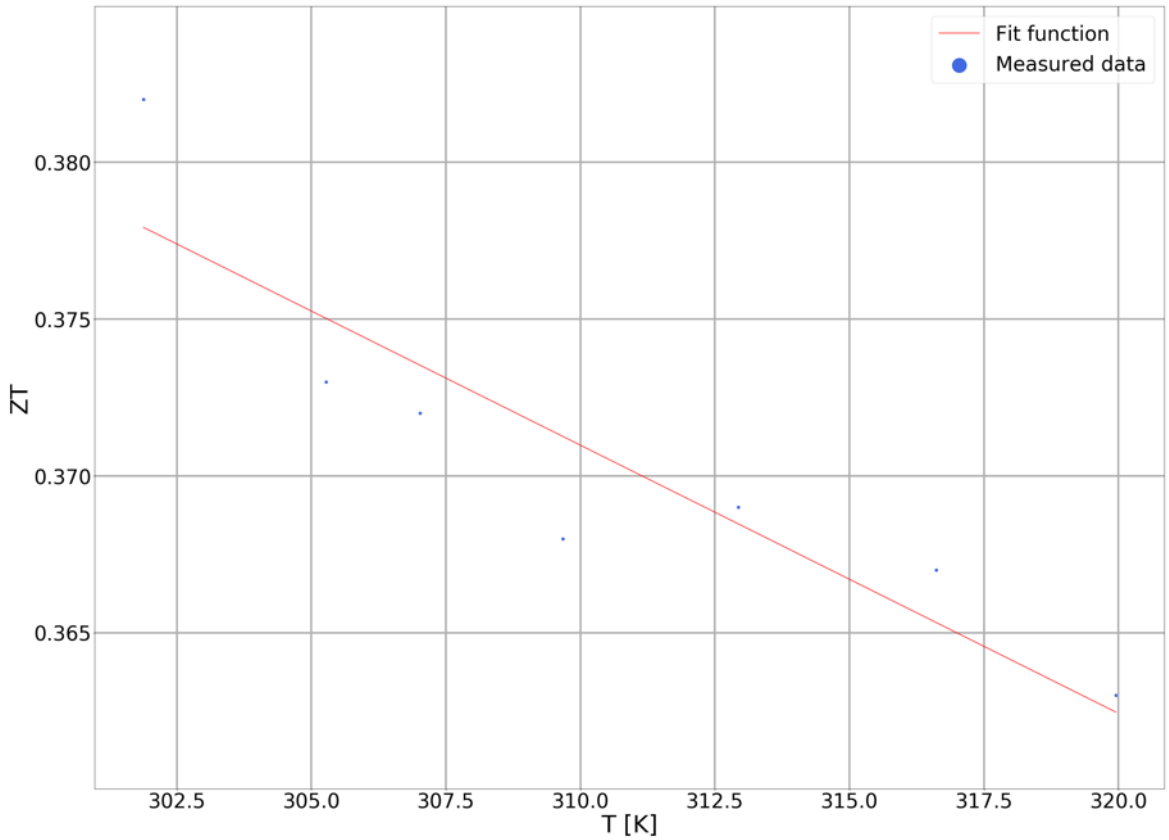

Figure 4.3: Fit function of ZT (cooling) with the data obtained from table 4.6.

4.2 Determination of ZT using the second method

The second method for determining ZT is more sophisticated in a sense that the temperature dependence can be shown directly using equation (2.43) in (2.33) as described in section 2.2. To repeat equation (2.43), because it is critical to determining ZT using the second method, it states that $\tau_{1,2}$ can be expressed as follows:

$$\tau_{1,2} = \frac{T_C - T_H(t)}{\dot{T}_H} \tag{4.8}$$

The derivative of the temperature with respect to time $\dot{T}_H$ has been obtained via numerical derivation. In order to reduce the noise, only every 20th data point has been used to obtain the derivation.
Only the process of cooling down has been considered for this method.

An example of a result of τ obtained using equation (4.8) can be seen in figure 4.4.

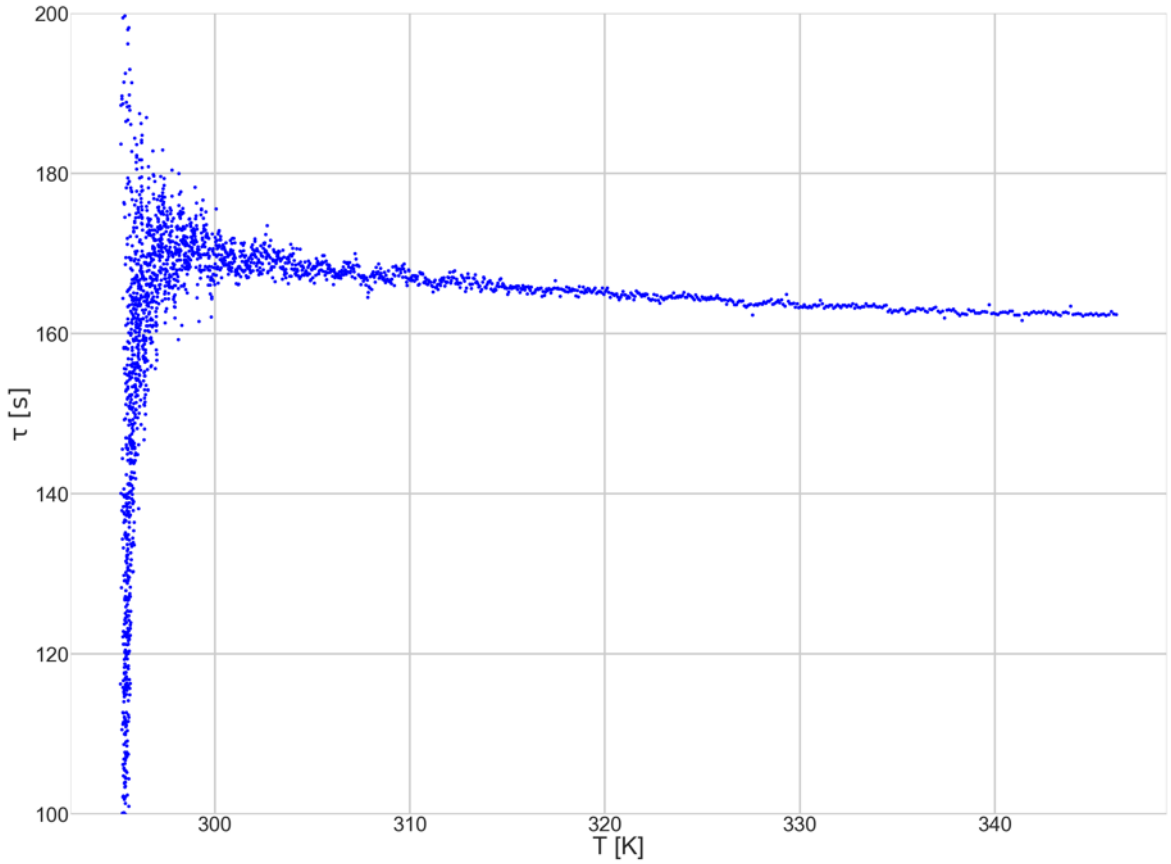

(a) Temperature dependent time constants τ with open circuit.

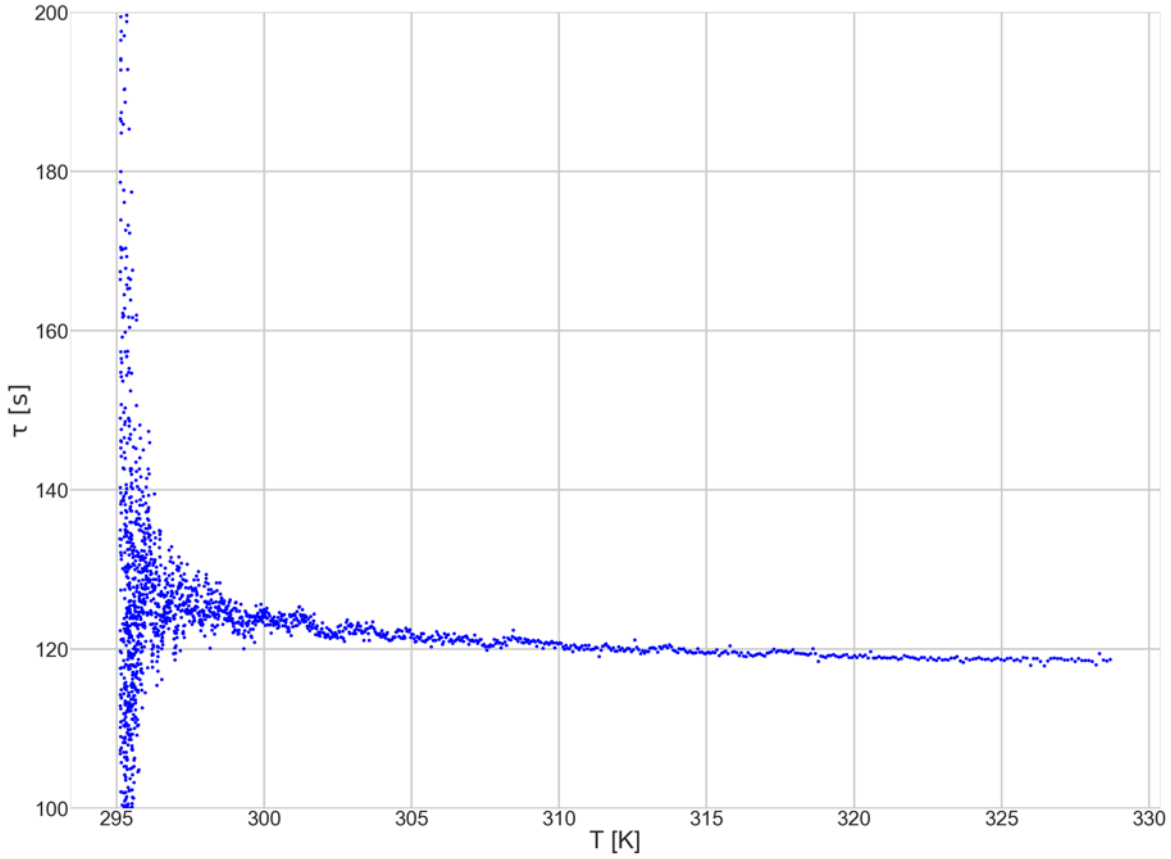

(b) Temperature dependent time constants τ with closed circuit.

Figure 4.4: Result of temperature dependent τ for measurement number 8.1.

At cool temperatures close to $T_H = 295K$, it can be seen that the scattering has an extremely wide range. This is most likely an artifact due to the numerical derivation done in equation (4.8).
Nevertheless, a clear decrease of τ can be seen as the temperature T_H rises. The combined results for measurements 1.1 to 8.1 can be seen in figure 4.5. No noticeable difference can be seen to the other set of measurements (measurement numbers 1.0 to 8.0), which is why I decided to not include their resulting figures here.

We can express the temperature dependence on τ if we prune the data seen in figure 4.5 such that the initial scattering is not included and fit a regression line through the remaining data. A good pruning point seems to correspond to all temperatures from $T_H > 310K$ on. The resulting fits can be seen in figure 4.6.

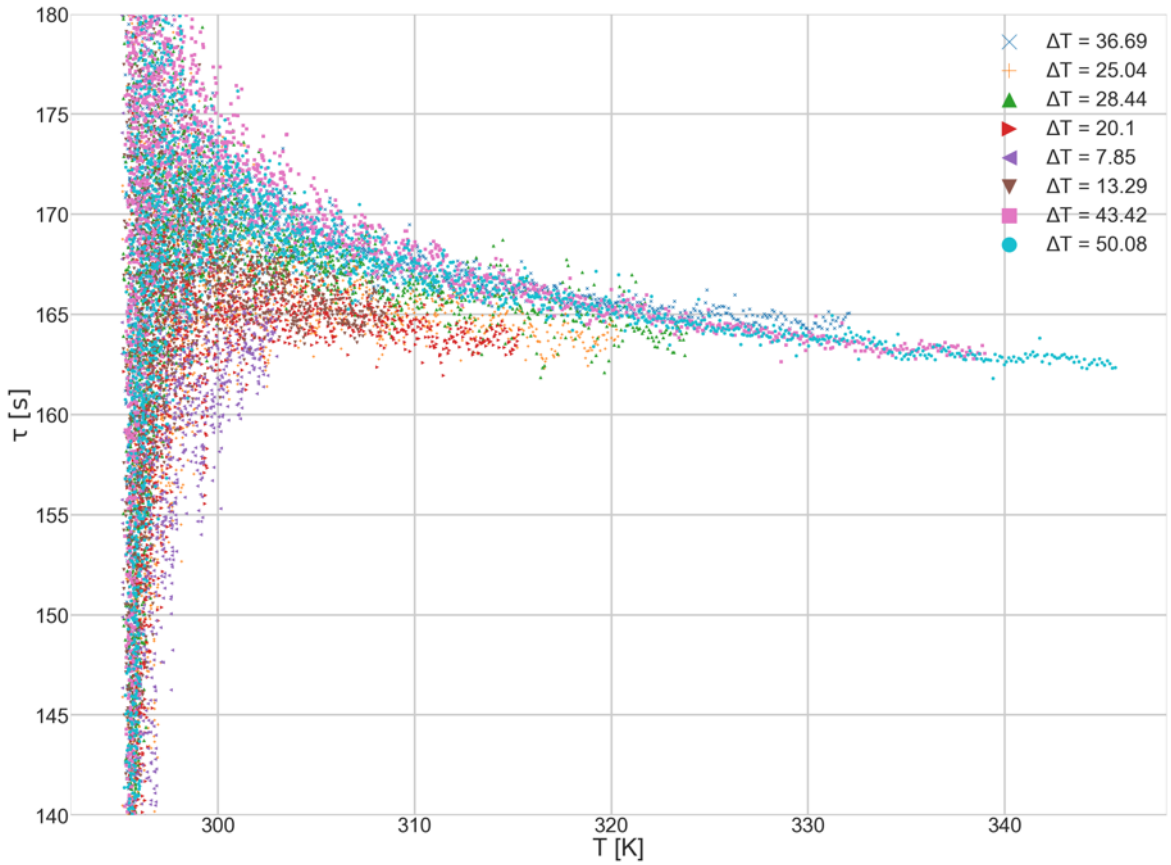

(a) Temperature dependent time constants τ with open circuit.

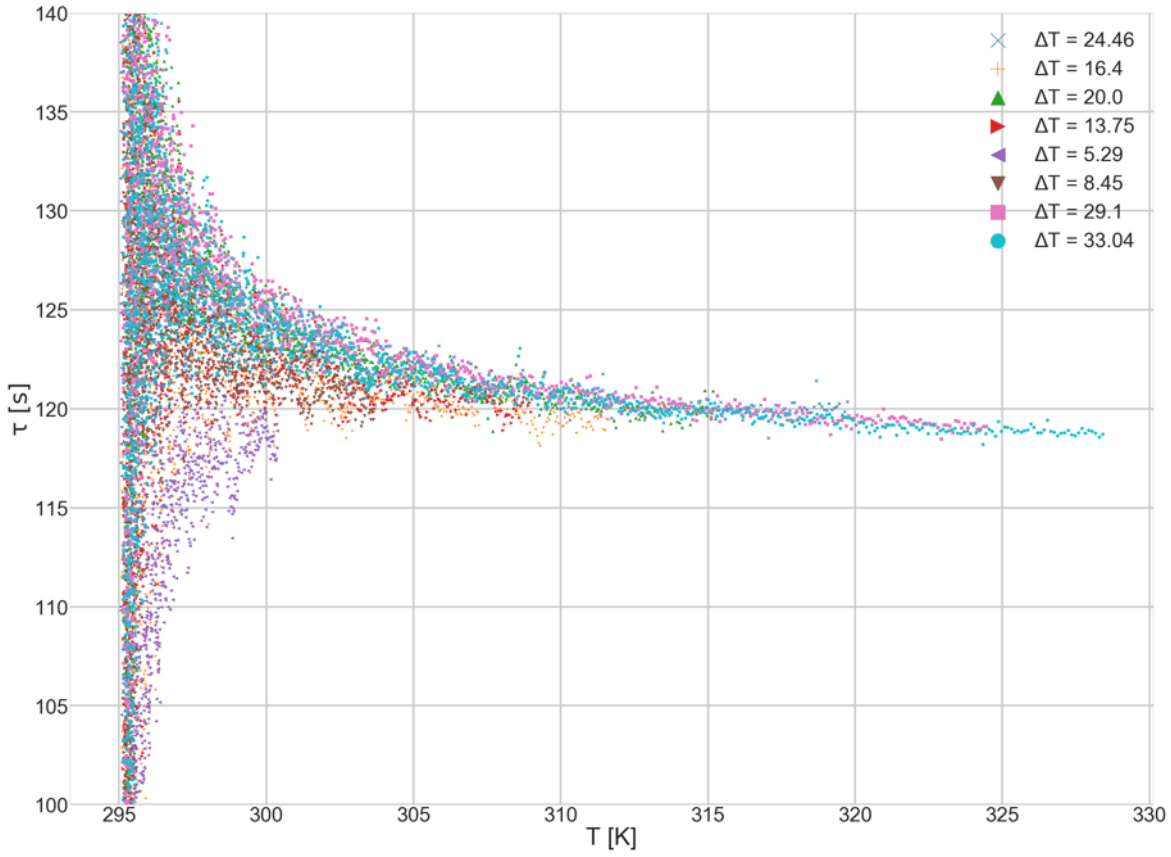

(b) Temperature dependent time constants τ with closed circuit.

Figure 4.5: Combined results of temperature dependent τ for measurements number 1.1 to 8.1.

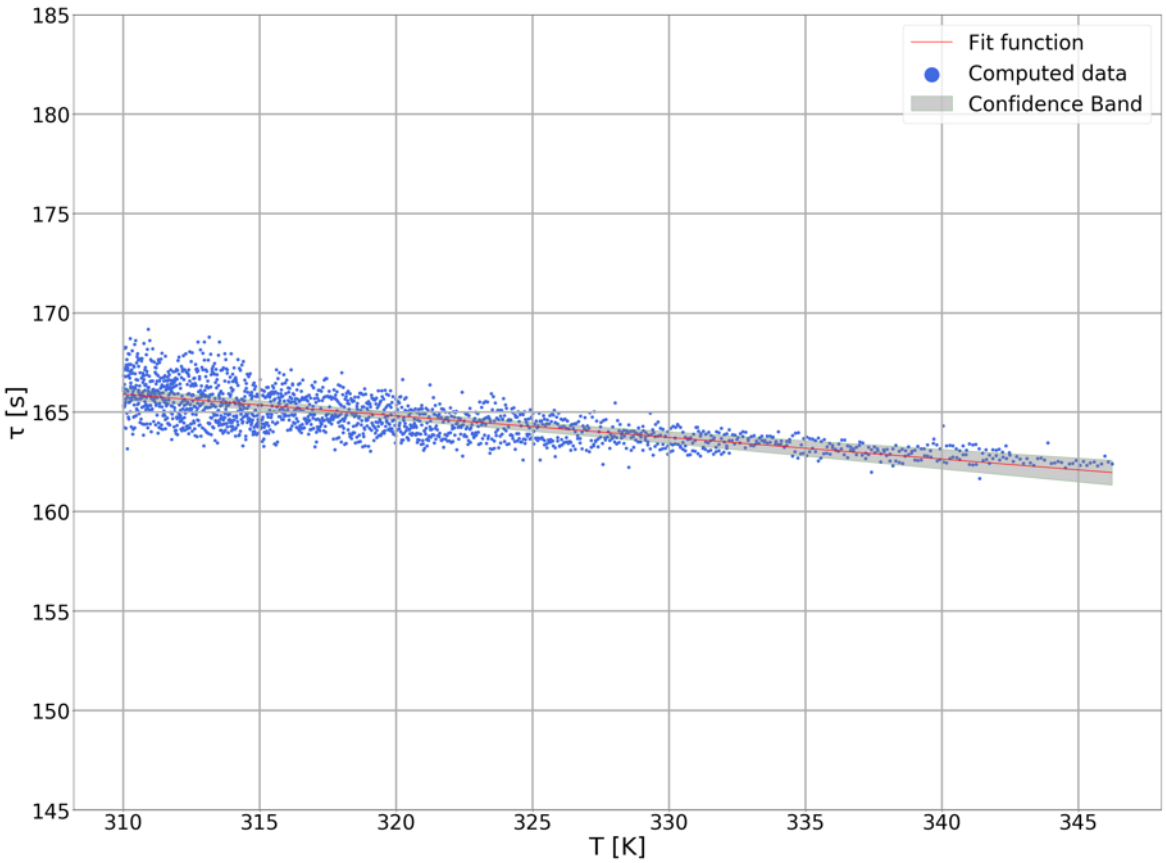

(a) Temperature dependent time constants τ_1 with open circuit, fitted with a linear regression line.

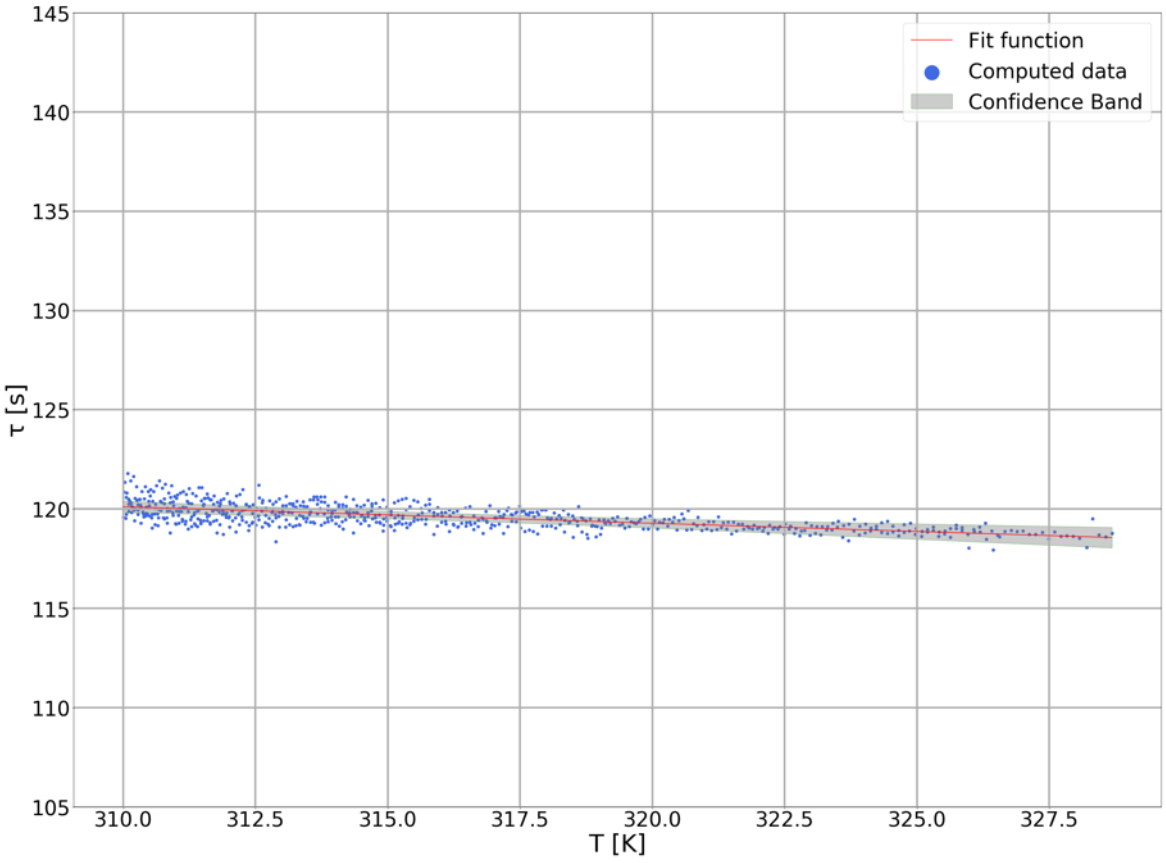

(b) Temperature dependent time constants τ_2 with closed circuit.

Figure 4.6: Fitted results of temperature dependent $\tau_{1,2}$ for measurements number 1.1 to 8.1. The grey area along the fit shows the confidence band, meaning it encloses the area in which we can be 95% sure that it contains the true curve [21].

The corresponding fit functions seen in figure 4.6 are as follows:

$$\tau_1(T) = -0.109 * T + 199.602 \pm 0.870[s] \tag{4.9}$$
$$\tau_2(T) = -0.083 * T + 145.848 \pm 0.455[s] \tag{4.10}$$

where the uncertainties have been obtained using the standard error of the estimate, also known as the root mean square error [22]. The uncertainty on the time constant with closed circuit τ_2 is smaller than that of τ_1, because the temperature T_H is considerably smaller when the thermoelectric cooler is active, meaning most of the initial scattering is cut off. This can also be seen in figure 4.7 when considering the fact that the scales of the x-axes are not the same in (a) and (b).

For the set of measurement 1.0 to 8.0 figures 4.6 (a) and (b) look almost identical which is why only the actual fit functions will be included. The fit functions for the other set of measurements are therefore as follows:

$$\tau_1(T) = -0.105 * T + 198.709 \pm 1.013[s] \tag{4.11}$$
$$\tau_2(T) = -0.097 * T + 150.417 \pm 0.414[s] \tag{4.12}$$

The temperature dependent ZT can now be computed using this data and equation (2.33). Since this is the most important result of this thesis, the graphical results for both sets of measurements of ZT have been included this time. The results can be seen in figure 4.7.

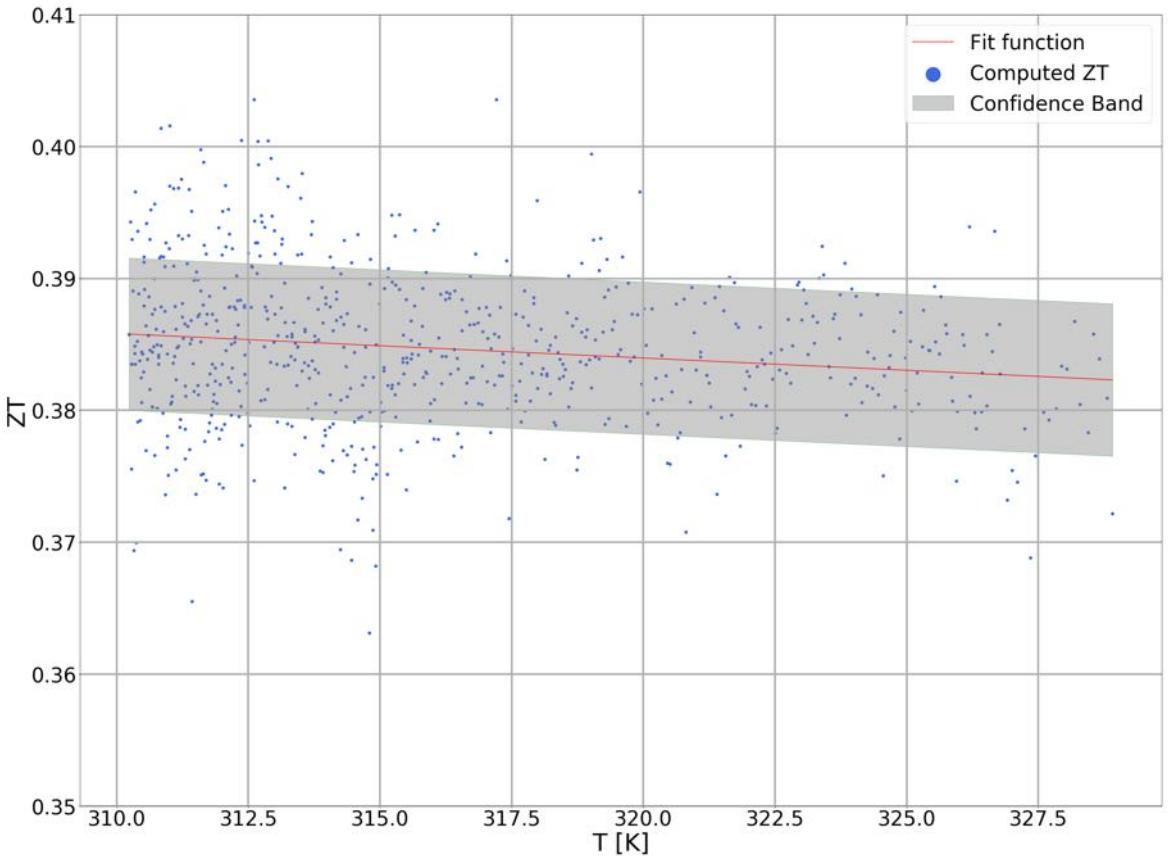

(a) Temperature dependent figure of merit ZT for the set of measurements 1.1 to 8.1.

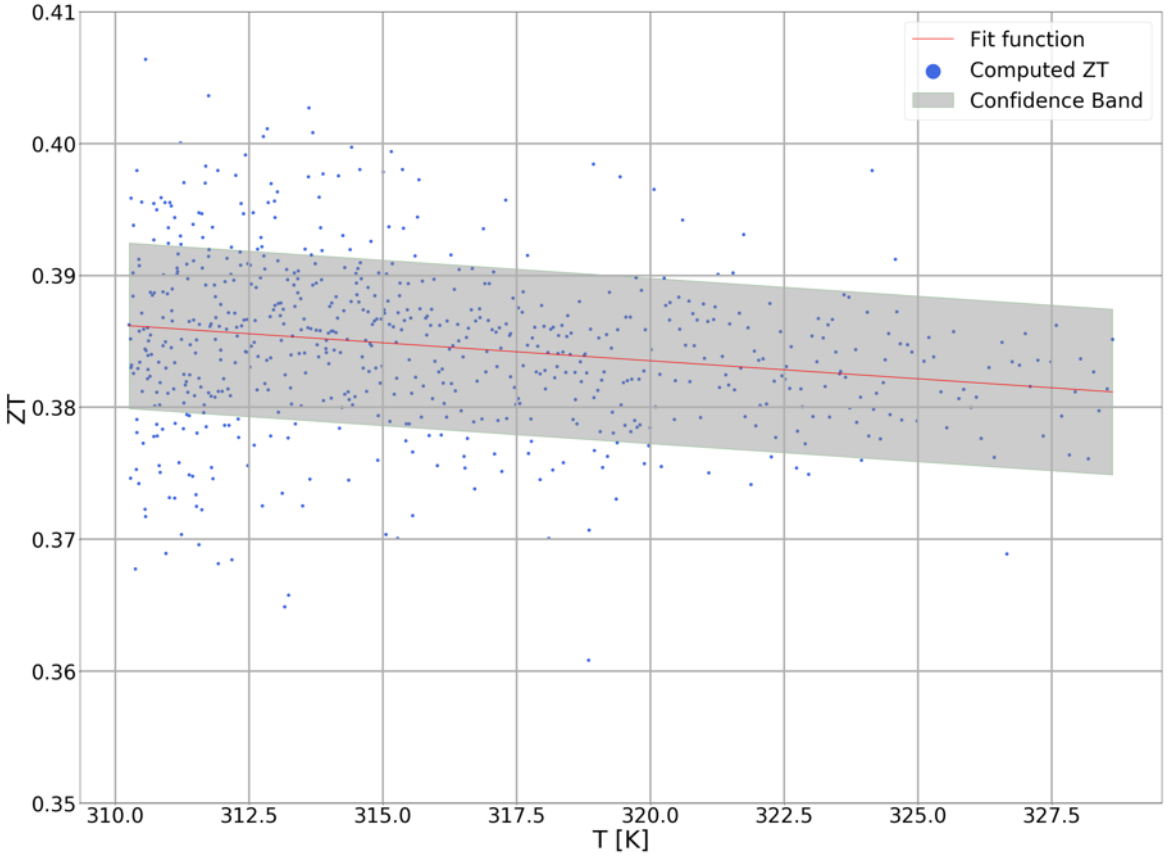

(b) Temperature dependent figure of merit ZT for the set of measurements 1.0 to 8.0.

Figure 4.7: Temperature dependent ZT for both sets of measurements.

The fit function from figure 4.7 (a) (measurements 1.1 to 8.1) is as follows:

$$ZT = -1.859 * 10^{-4} * T + 0.443 \pm 0.006 \tag{4.13}$$

For the other set of measurements (measurements 1.0 to 8.0) as seen in figure 4.7 (b), the fit function is:

$$ZT = -2.730 * 10^{-4} * T + 0.471 \pm 0.006 \tag{4.14}$$

It can be seen that equations (4.13) and (4.14) agree fairly well with each other. For a more accurate result, many more measurements would have to be done, however, this would be out of scope for this bachelor thesis.

The measurement set without paper inside the Styrofoam container should be different from this. In section 2.2, the assumption was made that all heat flows from the small copper body into the heat sink, implying perfect thermal insulation from the environment. This leads to believe that ZT obtained from measurements 1.2 to 8.2 should be further away from the true ZT than the results obtained before. It will be included anyways for the sake of completeness, the result can be seen in figure 4.8.

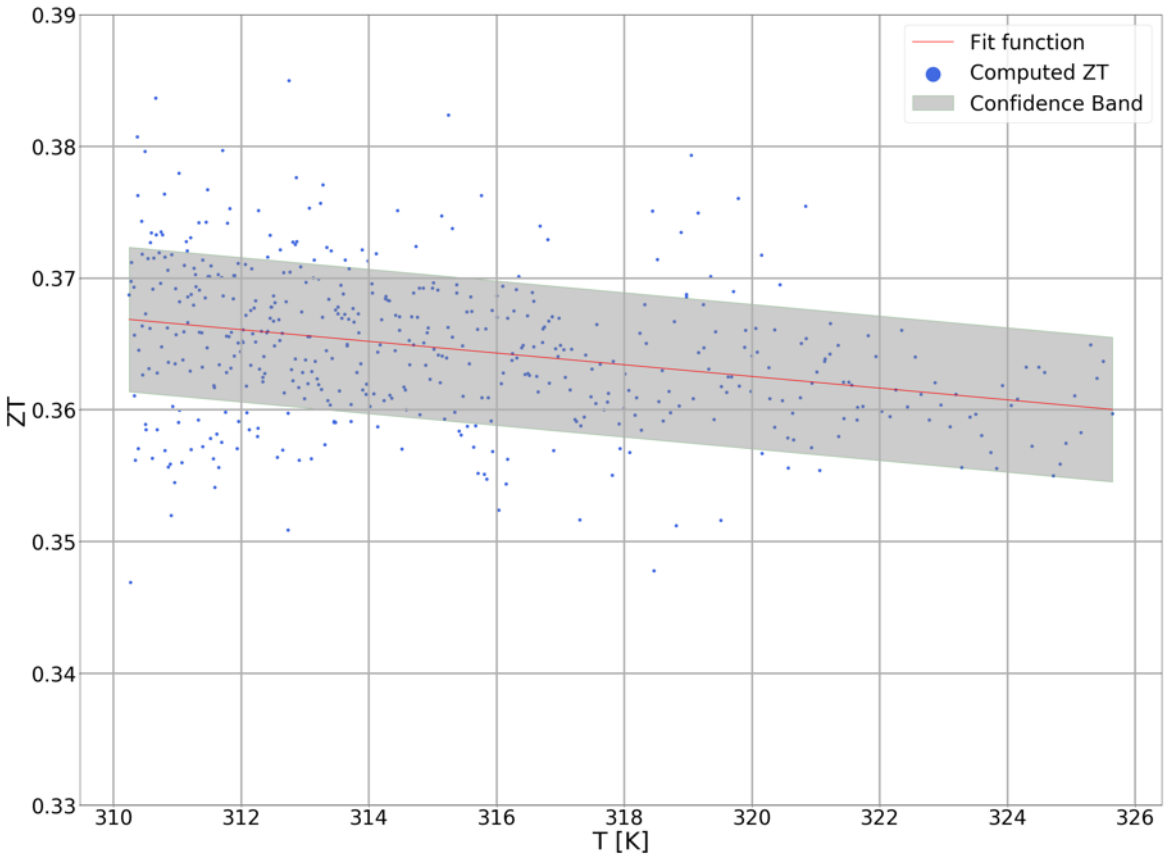

Figure 4.8: Temperature dependent ZT for the set of measurements 1.2 to 8.2, without paper inside the Styrofoam container.

It can already be seen that ZT has lower values compared to before. The fit function is as follows:

$$ZT = -4.438 * 10^{-4} * T + 0.505 \pm 0.005 \tag{4.15}$$

This is indeed a quite different result compared to equations (4.13) and (4.14).

4.3 Comparison to standard method for measuring ZT

In this section, we will compare the figures of merit obtained in sections 4.1 and 4.2 to the standard method for obtaining ZT, where α, k and R_{TE} are measured separately as described in section 3.4.
The result for the set of measurements 1.1 to 8.1 can be seen in table 4.7.

N	$\Delta T[K]$	α[V/K]	k[W/K]	R_{TE} [Ω]
1.1	11.51±0.01	$0.00282 \pm 3 * 10^{-6}$	0.0314	0.190±0.003
2.1	20.10±0.01	$0.00284 \pm 3 * 10^{-6}$	0.0321	0.200±0.003
3.1	28.84±0.01	$0.00287 \pm 3 * 10^{-6}$	0.0327	0.201±0.003
4.1	37.59±0.01	$0.00288 \pm 3 * 10^{-6}$	0.0330	0.208±0.003
5.1	44.58±0.01	$0.00289 \pm 3 * 10^{-6}$	0.0336	0.212±0.003
6.1	52.93±0.02	$0.00290 \pm 3 * 10^{-6}$	0.0337	0.218±0.003
7.1	69.18±0.02	$0.00292 \pm 3 * 10^{-6}$	0.0346	0.230±0.003
8.1	73.67±0.02	$0.00290 \pm 3 * 10^{-6}$	0.0346	0.233±0.003

Table 4.7: Results of α, k and R_{TE} of the first set of measurements with paper inside the Styrofoam container.

The rise of the Seebeck coefficient α with the temperature seems to be negligible while the rise for the thermal conductivity k and the internal electrical resistance R_{TE} according to the temperature seem quite high in comparison.
The uncertainty on α is the estimated error of the volt meter. The uncertainty on k was obtained by the uncertainty estimation of the voltmeter and the uncertainty on ΔT. k was obtained using equation (3.7) and its final uncertainty was obtained from the error propagation law, however, it is too small to display here. The internal electrical resistance of the thermoelectric cooler was obtained as described in the final part of section 3.4. Since it was measured using a separate setup, it was not possible to achieve the exact same temperature gradient as in the setup used to determine α and k.
To solve this issue, R_{TE} was fitted using a regression line. Afterwards T_H according to table 4.7 was used in the fit function to obtain the resistance values seen in the last row of the table. Its error stems from the uncertainty of the estimate (root mean square error).
The fit function for R_{TE} is as follows:

$$R_{TE}(T) = 0.0007 * T - 0.0283 \pm 0.0031[\Omega] \tag{4.16}$$

The graphical result of the internal electric resistance can be seen in figure 4.9.

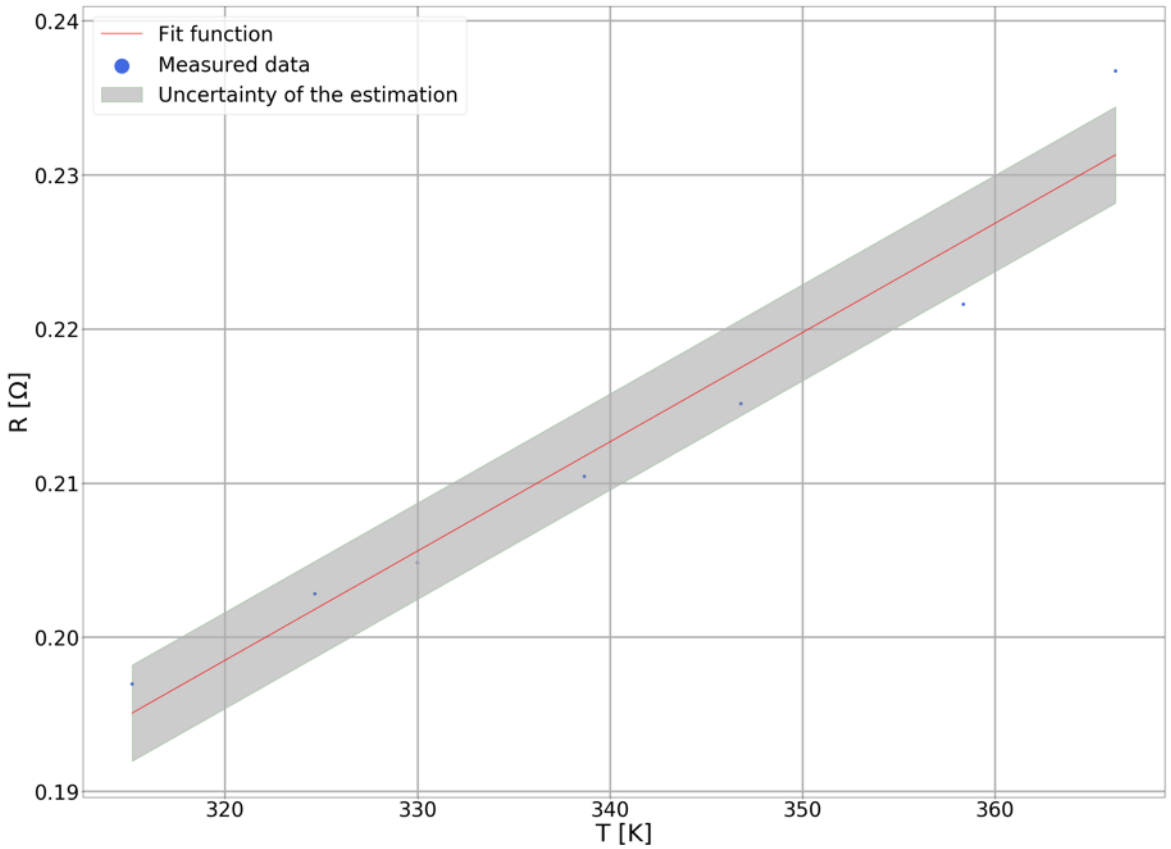

Figure 4.9: Temperature dependent R_{TE}. The grey area now represents the uncertainty of the estimation, as there are too few data samples for confidence bands to be reliable.

Finally, we are able to compute ZT using the definition of itself as seen in equation (1.3). The results can be seen in table 4.8:

N	ZT_{True}
1.1	0.412±0.006
2.1	0.407±0.006
3.1	0.405±0.006
4.1	0.403±0.006
5.1	0.398±0.006
6.1	0.396±0.005
7.1	0.391±0.005
8.1	0.389±0.005

Table 4.8: True values of ZT obtained through the standard method by measuring α, k and R_{TE} separately and using equation (1.3).

A clear decrease of ZT_{True} can be seen with rising temperature gradient ΔT. The error on ZT was obtained using the law of error propagation with the corresponding uncertainties from table 4.7. In order to compare these results to tables 4.4 and 4.6 from section 4.1, where ZT (cooling) is obtained by extracting the time constants $\tau_{1,2}$ from the exponential decay of $T_H(t)$, we require a temperature dependence on ZT_{True} first in order to be able to determine ZT_{True} at temperature T_{avg} from table 4.4. The temperature dependence on ZT_{True} is once again obtained by fitting a regression line using the data of table 4.8. The resulting fit function is as follows:

$$ZT_{True} = -3.337 * 10^{-4} * T + 0.514 \tag{4.17}$$

The graphical result can be seen in figure 4.10.

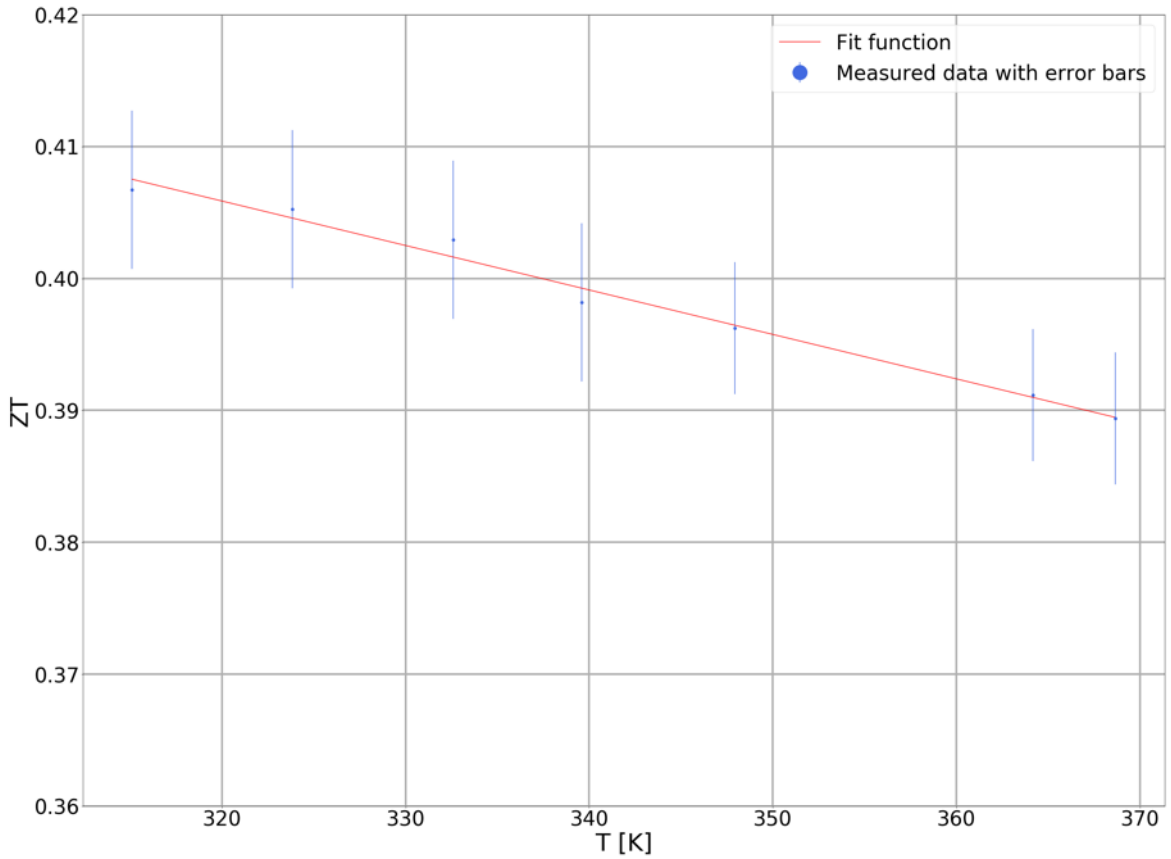

Figure 4.10: Temperature dependent ZT_{True} obtained by measuring α, k and R_{TE} separately.

Thus, we can use equations (4.17) and (4.7) at the temperatures T_{avg} seen in table 4.4 in order to directly compare the true values of ZT, ZT obtained by using the first new method with paper inside the Styrofoam container and lastly, ZT obtained by using the first new method without paper inside the Styrofoam container (equation (4.7)). The comparison can be seen in table 4.9.

T_{avg}	ZT_{True}	$ZT_{4.4}$	$ZT_{4.7}$
299.23±0.01	0.414±0.01	0.389	0.380±0.01
302.39±0.1	0.413±0.1	0.389	0.377±0.1
305.61±0.01	0.412±0.01	0.390	0.375±0.01
308.83±0.01	0.411±0.01	0.398	0.372±0.01
311.40±0.01	0.410±0.01	0.384	0.370±0.01
314.47±0.02	0.409±0.02	0.384	0.367±0.02
320.45±0.02	0.407±0.02	0.381	0.362±0.02
322.10±0.02	0.407±0.02	0.383	0.361±0.02

Table 4.9: True values of ZT from equation (4.17) compared to the values of ZT obtained by table (4.4) (with paper inside Styrofoam container) and equation (4.7) (without paper inside Styrofoam container).

It can be seen that these values of ZT_{True} do not agree with the values of ZT obtained via the first new method. They are too low, especially for the case where there was no paper inside the Styrofoam container.

Now we can compare the standard method for determining ZT to the second new method for determining ZT as seen in section 4.2. While the slope of equation (4.17) seems to agree reasonably well with equations (4.13) and (4.14), the intersection point seems quite a bit higher here. It is very likely that the temperature dependence of ZT_{True} is in fact not linear. This depends on the thermoelectric material [2].

Perhaps we can get a more conclusive comparison if we insert the temperatures for measurements 1.1 to 8.1 into the fit functions of ZT for the second method (equations (4.13) and (4.14)) and then compare these values to the values of ZT_{True} from table 4.8. The comparison can be seen in table 4.10 below.

N	ZT_{True}	$ZT_{4.13}$	$ZT_{4.14}$
1.1	0.412±0.006	0.386±0.006	0.387±0.006
2.1	0.407±0.006	0.384±0.006	0.385±0.006
3.1	0.405±0.006	0.383±0.006	0.383±0.006
4.1	0.403±0.006	0.381±0.006	0.383±0.006
5.1	0.398±0.006	0.380±0.006	0.380±0.006
6.1	0.396±0.005	0.378±0.006	0.376±0.006
7.1	0.391±0.005	0.375±0.006	0.372±0.006
8.1	0.389±0.005	0.374±0.006	0.370±0.006

Table 4.10: True values of ZT from table 4.8 compared to the values of ZT obtained by equation (4.13) and (4.14).

We notice a similarity with the first new method of obtaining ZT, which is that the second new method for obtaining ZT is closer to the true value of ZT the higher the temperature gradient. This statement only holds in the range of temperature gradients of our measurements, since the true temperature dependence most likely is not simply linear as mentioned before. It is not obvious what the true temperature dependence of ZT looks like for temperature gradients greater or smaller than those which appear in our measurements.

The values of ZT_{True} have also been measured for the case where there is no paper inside the Styrofoam container (measurements 1.2 to 8.2). The results of α, k and R_{TE} can be seen in table 4.11.

N	$\Delta T[K]$	α[V/K]	k[W/K]	R_{TE} [Ω]
1.2	11.24±0.01	$0.00282\pm3*10^{-6}$	0.0341	0.189±0.003
2.2	18.69±0.01	$0.00283\pm3*10^{-6}$	0.0351	0.193±0.003
3.2	27.91±0.01	$0.00287\pm3*10^{-6}$	0.0355	0.198±0.003
4.2	32.67±0.01	$0.00287\pm3*10^{-6}$	0.0358	0.201±0.003
5.2	40.68±0.01	$0.00290\pm3*10^{-6}$	0.0366	0.206±0.003
6.2	48.73±0.02	$0.00290\pm3*10^{-6}$	0.0372	0.211±0.003
7.2	58.73±0.02	$0.00292\pm3*10^{-6}$	0.0379	0.216±0.003
8.2	67.72±0.03	$0.00294\pm3*10^{-6}$	0.0385	0.222±0.003

Table 4.11: Results of α, k and R_{TE} of the set of measurements without paper inside the Styrofoam container.

The resulting values of ZT_{True} are again obtained by using the definition of ZT from equation (1.3) and can be seen in table 4.12.

N	ZT_{True}
1.2	0.404±0.006
2.2	0.391±0.006
3.2	0.390±0.006
4.2	0.380±0.006
5.2	0.385±0.006
6.2	0.380±0.005
7.2	0.371±0.005
8.2	0.382±0.005

Table 4.12: True values of ZT obtained through the standard method by measuring α, k and R_{TE} separately and using equation (1.3).

If we now fit a regression line for the data in table 4.12 in order to compare it to the second method for determining ZT, we obtain the following temperature dependence of ZT_{True}:

$$ZT = -2.721 * 10^{-4} * T + 0.475 \tag{4.18}$$

The graphical result can be seen in figure 4.11.

Comparing equation (4.18) to the first method for determining ZT (table 4.4 and equation (4.7)) by using the temperatures T_{avg} as seen in table 4.4, we arrive at a comparison as seen in table 4.13 below.

T_{avg}	ZT_{True}	$ZT_{4.4}$	$ZT_{4.7}$
299.23±0.01	0.394±0.01	0.389	0.380±0.01
302.39±0.1	0.393±0.1	0.389	0.377±0.1
305.61±0.01	0.392±0.01	0.390	0.375±0.01
308.83±0.01	0.391±0.01	0.398	0.372±0.01
311.40±0.01	0.390±0.01	0.384	0.370±0.01
314.47±0.02	0.389±0.02	0.384	0.367±0.02
320.45±0.02	0.388±0.02	0.381	0.362±0.02
322.10±0.02	0.387±0.02	0.383	0.361±0.02

Table 4.13: True values of ZT from equation (4.18) compared to the values of ZT obtained by table (4.4) (with paper inside Styrofoam container) and equation (4.7) (without paper inside Styrofoam container).

As can be seen, the values of ZT_{True} seem to agree very well with the values of $ZT_{4.4}$ which was obtained from the process of cooling down. The values of $ZT_{4.7}$, which were obtained from the measurement set without any paper inside the Styrofoam container are still quite different from ZT_{True}.

For the second new method, comparing equation (4.18) to (4.13) and (4.14), we see that they seem to be very similar. Especially remarkable is the fact that equation (4.18) is almost exactly the same as equation (4.14). However, equation (4.18) seems very different to equation (4.15) in which ZT which was obtained from the data where there was no paper inside the Styrofoam container.
A further comparison can be done again if we use the temperatures used to obtain ZT_{True} for table 4.11 in equations (4.13), (4.14) and (4.15). The comparison can be seen in table 4.14 below.

N	ZT_{True}	$ZT_{4.13}$	$ZT_{4.14}$	$ZT_{4.15}$
1.2	0.404±0.006	0.386±0.006	0.387±0.006	0.369±0.005
2.2	0.391±0.006	0.385±0.006	0.385±0.006	0.366±0.005
3.2	0.390±0.006	0.383±0.006	0.383±0.006	0.362±0.005
4.2	0.380±0.006	0.382±0.006	0.382±0.006	0.360±0.005
5.2	0.385±0.006	0.381±0.006	0.379±0.006	0.356±0.005
6.2	0.380±0.005	0.379±0.006	0.377±0.006	0.352±0.005
7.2	0.371±0.005	0.377±0.006	0.374±0.006	0.348±0.005
8.2	0.382±0.005	0.376±0.006	0.372±0.006	0.344±0.005

Table 4.14: True values of ZT from table 4.11 compared to the values of ZT obtained by equation (4.13), (4.14) and (4.15).

As can be seen, the ZT obtained from the data where there was paper inside the Styrofoam container (equations (4.13) and (4.14)) are within the error of margin of ZT_{True} for all measurements except measurement 1.2 which had the lowest temperature gradient.
The values of $ZT_{4.15}$ do not fit into this at all, they are quite different from the other values of ZT. This makes sense, considering we assumed that all heat exclusively flows from the small copper body to the heat sink in section 2.2. More heat is lost to the environment in the case of $ZT_{4.15}$ due to worse thermal insulation.

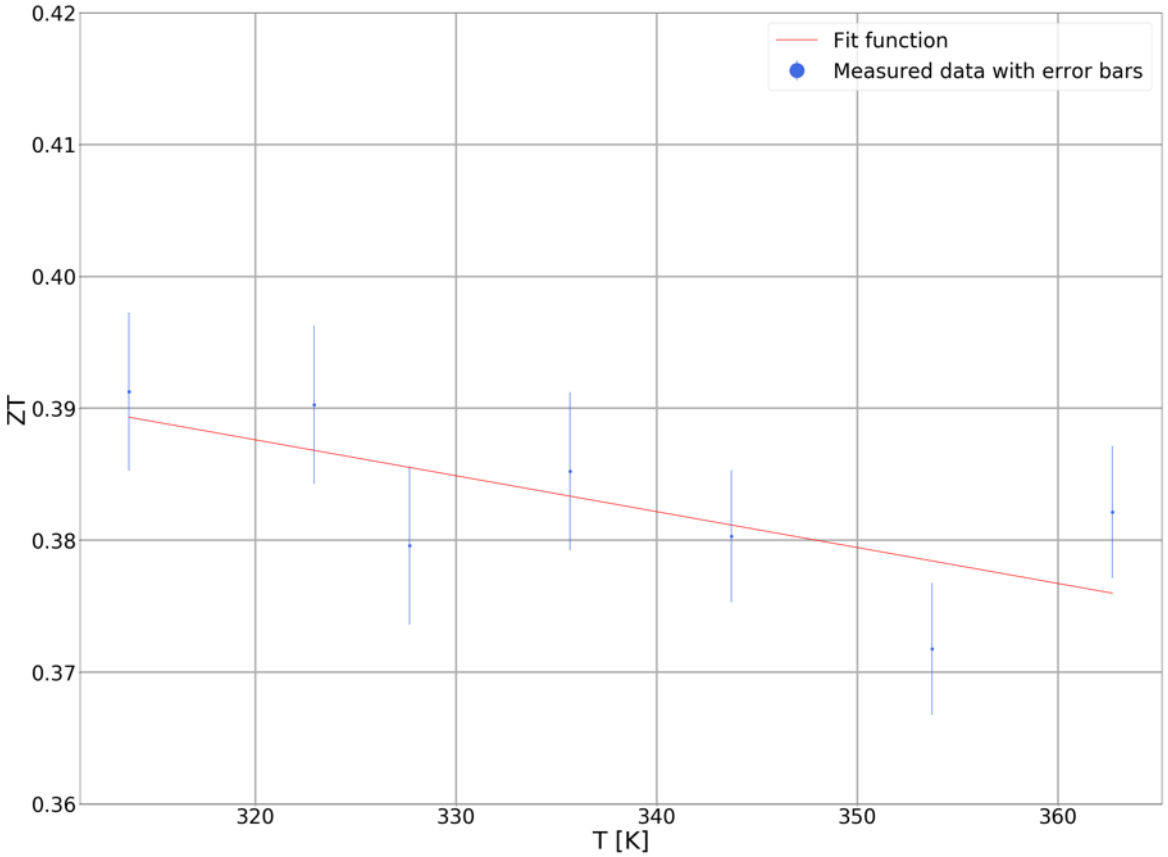

Figure 4.11: Temperature dependent ZT, without paper inside the Styrofoam container, obtained by measuring α, k and R_{TE} separately.

The fact that ZT_{True} obtained from the data with paper inside the Styrofoam container is further away from the ZT obtained via the new methods than the ZT_{True} obtained without paper inside the Styrofoam container might stem from the fact that the thermal conductivity k changes a lot depending on whether there is paper inside

the Styrofoam container or whether there is not. It might be that by adding paper into the Styrofoam container, we falsify the true value of ZT_{True} due to the change of k. The opposite is true for the values of ZT obtained via the second method, as described in section 2.2. The more thermal insulation we have, the closer the values of ZT should be to ZT_{True}. This might explain this discrepancy.

As a final comparison, the fit functions of all figures of merit ZT which were discussed in this section will be shown in figure 4.12 below.

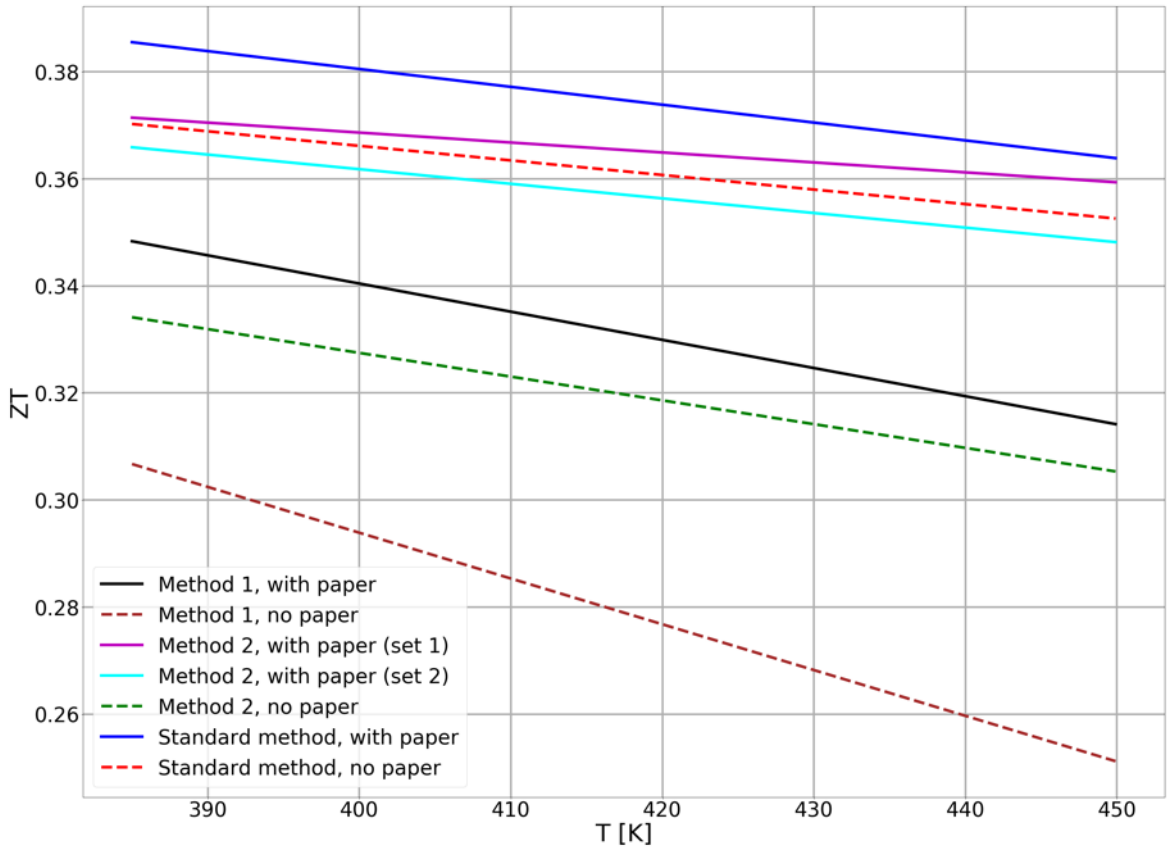

Figure 4.12: Comparison of all fits of ZT which were discussed above. The legend refers to the corresponding method. The line is dashed for the measurement sets where there was no paper inside the Styrofoam container. The red dashed line (equation (4.18)) is the fit for the values of the true ZT without paper inside the Styrofoam container. This is the reference for the other values of ZT. The black line (equation (4.4)) is the first new method for determining ZT, with paper inside the Styrofoam container. It can be seen that this is quite off from the true values of ZT (in red). The brown dashed line (equation (4.7)) is the first new method for determining ZT, without paper inside the Styrofoam container. This fit is the furthest away from the true values of ZT. The purple line (equation (4.13)), is the second new method for determining ZT. It is the first set of measurements with paper inside the Styrofoam container. As can be seen, it is very close to the true values of ZT. The cyan colored line (equation (4.14)) is also the second new method for determining ZT. It is the second set of measurements with paper inside the Styrofoam container. This one is the closest one to the true value of ZT, having almost the same slope but a slightly different offset. The green dashed line (equation (4.15)) is the second new method for determining ZT without paper inside the Styrofoam container. It is quite far away from the true values of ZT. The blue line (equation (4.17)) is the "true" value of ZT with paper inside the Styrofoam container. It is most likely not the actual true ZT for reasons discussed in this section.

4.4 Determination of ZT using the third method

This brings us to the last new method for obtaining ZT. It is described in section 2.3 and ZT is obtained by using equation (2.53). To repeat this equation, it states the following:

$$ZT = \frac{R_{eff}}{R_{TE}} - 1 \tag{4.19}$$

The effective electrical resistance is obtained by simply driving a current I through the thermoelectric cooler and measuring the resulting voltage V_{eff}. R_{eff} is then obtained as follows:

$$R_{eff} = \frac{V_{eff}}{I} \tag{4.20}$$

This has only been done for one current since a measurement for this method takes a very long time. The current driven through the thermoelectric cooler and the corresponding measured voltage V_{eff} are as follows:

$$I = 0.0981A \tag{4.21}$$
$$V_{eff} = 0.0313V \tag{4.22}$$
$$R_{eff} = 0.3191\Omega \tag{4.23}$$

Using equation (1.1) to convert the voltage to a temperature (assuming $\alpha \approx 0.0028V/K$) we get:

$$T_H - T_C = \frac{V_{eff}}{\alpha} \tag{4.24}$$
$$T_H = \frac{V_{eff}}{\alpha} + T_C \tag{4.25}$$
$$T_H = 307.52K \tag{4.26}$$

In order to then determine the corresponding R_{TE}, the temperature obtained above can be inserted into equation (4.16). We get:

$$R_{TE} = 0.187\Omega \tag{4.27}$$

Finally, we can insert all the necessary values into equation (4.19) to obtain ZT:

$$ZT = 0.706 \tag{4.28}$$

This value of ZT is very different from any of the values obtained before, thus, this method is unsuited for the determination of ZT. My assumption is that it is very hard to get a precise measurement using this experimental setup as the current driven through the thermoelectric cooler and the corresponding measured voltage still kept fluctuating even after waiting for multiple hours.

As a bonus, I decided to check whether R_{TE} can be obtained using equation (2.55). To repeat it, it states that R_{TE} can be expressed as follows:

$$R_{TE} = R_{eff}\frac{\tau_2}{\tau_1} \tag{4.29}$$

Using the temperature obtained in equation (4.26), it is possible to determine the corresponding τ_1 and τ_2 using equations (4.9) and (4.10). We get:

$$\tau_1 = 166.082s \tag{4.30}$$

$$\tau_2 = 120.234s \tag{4.31}$$

For R_{eff}, I decided to compute it from equation (2.52) instead of taking the value which was measured directly as it was deemed too unprecise. We get:

$$R_{eff} = R_{TE}(1 + ZT) \tag{4.32}$$

Inserting equations (4.28), (4.30) and (4.31) into (4.29), we get:

$$R_{TE} = 0.258\Omega \tag{4.33}$$

This is quite different from R_{TE} obtained in equation (4.27), although I believe that if R_{eff} had a higher precision, it would work out quite well.

Conclusion

It was shown in theory and experimentally that there are two new methods for effectively measuring the figure of merit ZT in one single experiment. Both methods require the same setup, namely a temperature gradient between the body which is to be cooled and the heat sink. After a temperature gradient has been established, a measurement of the temperature decay has to be taken once when the thermoelectric cooler is inactive and once when it is active. This will yield two different time constants with which it is possible to determine the figure of merit ZT.

The first new method for determining ZT seems to agree reasonably well with the values of ZT_{True}, obtained via the standard method for measuring ZT. However, only the measurements taken during the cooling process and with sufficient thermal insulation seem to agree with ZT_{True}. The fit function of ZT obtained via the first method generally seem too low as seen in figure 4.12.

The second new method for determining ZT seems not only more accurate than the first new method, but it also shows a direct temperature dependence. The results are within the margins of error compared to ZT_{True}, except for the measurement with the lowest temperature gradient. Again, sufficient thermal insulation is necessary for the results to be accurate.

The third new method for determining ZT seems impractical and inaccurate, although I believe that it could still be done by having much more precise measurements.

Acknowledgements

I would like to thank Prof. Dr. Andreas Schilling for giving me the opportunity to work in his group. He also supervised me during my work and was tremendously helpful whenever I needed anything. It was a pleasure to work with him and I feel like I learned a lot. I would also like to thank the physics workshop at the UZH for their support.

References

1. Seebeck, T.J. Abhandlungen der Königlichen Akademie der Wissenschaften zu Berlin. 265 (1823)

2. Tritt, T. M. Subramanian, M. A. Thermoelectric Materials, Phenomena, and Applications: A Bird's Eye View. MRS Bull. 31, 188–198 (2006).

3. Peltier, J.C. Ann. Chem. 371 (1834).

4. Kittel, C. Introduction to solid state physics. 142-207 (Wiley, 2005).

5. Pradip Basnet. Metal Oxide Photocatalytic Nanostructores Fabricated By Dynamic Shadowing Growth. 9-11 (2015).

6. Föll, Helmut. Thermoelectric Effects. (2019). at <https://www.tf.uni-kiel.de/matwis/amat/elmat_en/kap_2/advanced/t2_3_2.pdf>

7. Hangsubcharoen, M. A Study of Triboelectrification for Coal , Quartz and Pyrite. 55-58 (Virginia Polytechnic Institute and State University, 1999).
8. Lundstrom, M. Lecture 10: Thermoelectric Effects: (electronic) heat flow. 10-15 (2011).

9. Goldsmid, H. J. Thermoelectric Refrigeration. 13-14 (Springer US, 1964).

10. Schilling, A., Zhang, X. Bossen, O. Heat flowing from cold to hot without external intervention by using a "thermal inductor". Sci. Adv. 5, eaat9953 (2019).

11. Zhang, X. Zhao, L.-D. Thermoelectric materials: Energy conversion between heat and electricity. Journal of Materiomics 1, 92–105 (2015).

12. Jangonda, C. et al. Review of Various Application of Thermoelectric Module. 5, 8 (2007).

13. Bowley, A. E., Cowles, L. E. J., Williams, G. J. Goldsmid, H. J. Measurement of the figure of merit of a thermoelectric material. J. Sci. Instrum. 38, 433–435 (1961).

14. Goupil, C., Seifert, W., Zabrocki, K., Müller, E. Snyder, G. J. Thermodynamics of Thermoelectric Phenomena and Applications. Entropy 13, 1495 (2011).

15. Demtröder, W. Experimentalphysik 2. 55 (Springer Berlin Heidelberg, 2013).

16. Zhang, D.-B., Li, H.-Z., Zhang, B.-P., Liang, D. Xia, M. Hybrid-structured ZnO thermoelectric materials with high carrier mobility and reduced thermal conductivity. RSC Adv. 7, 10855–10857 (2017).

17. Lienhard, J. H. Lienhard, J. H. A Heat Transfer Textbook. 6-10 (Dover Publications, 2011).

18. Demtröder, W. Experimentalphysik 1. 274 (Springer Berlin Heidelberg, 2018).

19. Jeon, H.-G., Song, J. Y., O, B. Kim, Y.-G. Measurement of electrical resistance of thermoelectric materials with a temperature gradient using instant load-voltage analysis. Meas. Sci. Technol. 29, 095601 (2018).

20. Young, P. Everything you wanted to know about Data Analysis and Fitting but were afraid to ask. arXiv:1210.3781 [cond-mat, physics:physics] (2014).

21. GraphPad. Confidence and prediction bands. at <https://www.graphpad.com/guides/prism/latest/curve-fitting/reg_confidence_and_prediction_band.htm>

22. Nau, Robert. Mathematics of simple regression. at <https://people.duke.edu/~rnau/mathreg.htm>